SUPPORTING INFORMATION

Mustroph et al. 10.1073/pnas.0906131106

Supporting Results

Cell/Region-Specific Polysomal mRNA Populations Are Distinct. The data presented here indicate that cell/region-specific mRNA-ribosomes populations (translatomes) can be reproducibly isolated from individual cell types based on the use of cell- and region-specific promoters to drive *FLAG:RPL18* in Arabidopsis. The high correlation coefficients of Robust Multi-chip Average (RMA) signal values between biological replicates (r^2 = 0.93-0.99; Dataset S1, sheet *g*) indicate that the immunopurification method is highly reproducible. This reproducibility extends to cell types that are a minor component of the organ, such as phloem companion cells (CC) and guard cells. Accordingly, hierarchical clustering of the RMA expression data revealed close proximity of replicates (Fig. S14). This basic clustering method confirmed that translatomes were distinguishable first by organ, then by growth condition and finally by cell type, leading to the conclusion that gene expression changes due to hypoxia were more pronounced than cell-type differences. This also showed that some shoot cell types [*i.e. pSUC2* (phloem CC), *pCER5* (epidermis)] still differed from each despite the reconfiguration of translation during the stress treatment.

***pGL2* and *pSultr2;2* Promoter Specificity.** Although most translatomes were consistent with expectations for the targeted cell types, *pGL2* and to a lesser extend *pSultr2;2* showed limited mRNA specificity. *pGL2* was expected to be localized in root atrichoblasts (*1*) and shoot trichomes (*2*). However, root *pGL2* mRNAs overlapped with those of *pSultr2;2* and *pSUC2* (Datasets S2 and S3, Fig. S5). There were only 33 genes significantly lower and 59

genes higher in *pGL2* than in *pSultr2;2* roots, and 52 and 94 genes in shoots, respectively, and *pGL2* and *pSultr2;2* samples clustered close together (Fig. S14). Confocal imaging of over 50 independent *pGL2:GFP-RPL18* transgenics confirmed expression of this promoter in atrichoblasts, but also revealed a low activity in the root vasculature (Fig. S1*B*). In aerial tissue, *pGL2* produced GFP-tagged ribosomes in trichomes and epidermal cells at the petiole base (Fig. S1*A*). Although 20 *pGL2*-enriched mRNAs were associated with epidermal-specific expression, 32 mRNAs were enriched in the phloem CC population (Dataset S2, sheet c). *pSultr2;2* transgenics showed expression limited to the vasculature in roots and shoots (Fig. S1*C*), but the overlap with shoot *pSUC2*-enriched mRNAs was lower than expected, whereas photosynthesis-associated mRNAs were elevated (Datasets S2 and S3). This pattern of mRNA enrichment is consistent with the documentation of *pSultr2;2* expression in shoot bundle sheath cells (*3*). The *pGL2* and *pSultr2;2* promoters may provide less unique mRNA populations because of expression in multiple cell types, emphasizing that promoters with robust expression are most desirable for cell-specific expression analyses. We treated the *pGL2* and *pSultr2;2* mRNA populations in the analysis of differentially expressed genes as they behaved in the microarray dataset and the GFP-tagged ribosome analysis, and not as predicted from the literature.

Distribution of Ribosomal Protein mRNAs Within Cell Types and Organs. Fuzzy k-means clustering of cell-type specific mRNAs under control conditions revealed two clusters enriched in ribosomal proteins (Fig. S5*B*; Dataset S3). The mRNAs encoding ribosomal proteins and translation factors were strongly enriched in clusters 38 (6.14E-56; 4.09E-33) and 77 (9.68E-19; 6.75E-08). Strikingly, mRNAs encoding components of the protein synthesis apparatus were depleted in the proliferating cells of the root (*pRPL11C*),

phloem CC (*pSUC2*) and maturation zone of the root cortex (*pPEP*). The low levels of ribosomal protein mRNAs in polysomes in the *pRPL11C* population was unexpected but provides further evidence that this cohort of mRNAs is translationally regulated in plants as observed in animals (*4-6*). Accordingly, reduced translation of ribosomal protein mRNAs was evident in most cell types of the root and shoot in response to hypoxia (cluster 58; Fig. S10*B*).

Supporting Materials and Methods

Generation of *promoter:HF-RPL18* and *promoter:HF-GFP-RPL18 Arabidopsis thaliana* Transgenic Lines. The T-DNA binary vector pPZP111 (*7*) containing the CaMV 35S promoter and OCS3' terminator (pS119) was modified by replacement of the promoter region with the Gateway recombination cassette att1-cmR-ccdb-att2 (Invitrogen) by use of the *Eco*RI and *Sac*I sites to produce pGATA-S119. The tobacco mosaic virus (TMV) omega 5' leader-HF-RPL18B (At3g05590) cassette described by Zanetti et al., (*8*) was amplified by standard polymerase chain reaction (PCR) to replace the *Sac1* with *Kpn1* (primers see Table S1) so that the product could be inserted into the *Kpn*I and *Xba*I sites of pGATA-S119 (Fig. S1). The resultant vector construct, pGATA:HF-RPL18, was used for recombinational insertion of cell-type specific promoters upstream of the HF-RPL18 coding sequence. This construct includes the TMV omega 5' leader (66-bp) fused to an open reading frame that consists of $M(H)_6(G)_3$DYKDDDDK(the FLAG epitope)$(G)_7$ fused the 187 amino acid coding sequence of *RPL18B*.

The coding sequence of sGFP (*9*) was amplified from a plasmid (pCsGFPBT, GenBank accession: DQ370426), using forward primer GBamHIF: 5'- GAC TGG ATC CAT GGT GAG CAA GGG CGA GGA G -3' and reverse primer GBamHIR: 5'- GTC

AGG ATC CCT TGT ACA GCT CGT CCA TGC C -3'. The PCR product was digested with restriction enzyme *Bam*HI and inserted into p35S:HF-RPL18 (*8*) to form an in-frame fusion of p35S:HF-sGFP-RPL18. Additionally, a Gateway vector was constructed as follows: the TMV 5' leader-His_6FLAG-GFP-RPL18B cassette from p35S:HF-sGFP-RPL18 was amplified by PCR using primers as described for pGATA:HF-RPL18. The PCR product and the vector pGATA:HF-RPL18 were digested with *Kpn*I and *Xba*I and ligated to form pGATA:HF-sGFP-RPL18. Maps of these construct are provided in Fig. S1 at the end of this section.

The destination vectors with gene 5' flanking regions were constructed as follows: promoter sequences were amplified by PCR from Arabidopsis genomic DNA by use of primers designed to bind just 5' of the initiator methionine and at the boundary of the nearest 5' gene. Forward primers had an additional 5'-CACC (Table S1). The amplified DNA fragments were cloned into the pENTR/D-TOPO vector (Invitrogen, Carlsbad, CA, USA). Following recombination into pGATA:HF-RPL18 or pGATA:HF-sGFP-RPL18, the sequence of the promoter and coding region were verified by cycle sequencing (Institute for Integrated Genome Biology Core Facility, University of California, Riverside). Binary T-DNA vectors were electroporated into *Agrobacterium tumefaciens* (strains LBA4404 (*pGATA:HF-RPL18*) or GV3101 (*pGATA:HF-sGFP-RPL18*)) and 6-wk-old *Arabidopsis thaliana* ecotype Columbia (*Col-0*) plants were transformed by the floral dip method (*10*). Transgenic lines were identified by selection on solid MS medium for kanamycin resistant seedlings and propagated on soil as previously described (*8*). Plants were cultivated in a growth chamber at 22 °C under long-day photoperiod (16 h 200 μE m^{-2} s^{-1} light). The RPL18B fusion includes the His_6 and FLAG tags, but is referred to FLAG-RPL18 in the subsequent text.

Establishment and Characterization of *p:FLAG-RPL18* Transgenics with a Single T-DNA Insertion. FLAG-RPL18 expressing transgenic lines were identified by immunoblot analyses of crude seedling tissue extracts or by immunoprecipitation of the FLAG-tagged protein as described previously (*8*). Lines that showed an average level of positive expression were selected for further study. No abnormalities in seedling growth, plant development or fecundity were observed in the *p:FLAG-RPL18* transgenics. Lines were further characterized by evaluation of the copy number of T-DNA insertions and ultimately the site of insertion. Genomic DNA was isolated from rosette leaves from third-generation (T3)-plants as follows: 2 mL of frozen pulverized tissue was homogenized in 10 mL DNA Extraction Buffer [0.5 M NaCl, 200 mM Tris-HCl, pH 8.0, 100 mM EDTA, 2% (w/v) SDS], incubated at 65 °C for 30 min, extracted with one volume of chloroform-isoamyl alcohol (24:1), and centrifuged at 4,000 *g* for 15 min. The DNA in the supernatant was concentrated by isopropanol precipitation, and resuspended in 1 mL of 10 mM Tris-HCl, pH 8.0, 1 mM EDTA, containing RNAse. After incubation for 30 min at 37 °C, the solution was extracted with phenol, and precipitated with ethanol. T-DNA insertion copy number in each candidate line was determined by Southern blot analysis by digestion of genomic DNA (20 µg) with *Eco*RI, *Bam*HI or *Xba*I, transfer to nylon membranes and hybridization with an *OCS3'* fragment. For each *p:FLAG-RPL18* construct a line with a single site of T-DNA integration (or two sites in case of *pCER5*) was established. The site of T-DNA insertion was determined by thermal asymmetric interlaced PCR (TAIL-PCR) using arbitrary degenerate (AD) primers and three successive primers each from the left or right border of T-DNA (Table SI) essentially as described in ref. *11*. TAIL-PCR products from the third amplification cycle were purified from an agarose gel by use of the QIAprep gel

purification kit (Qiagen) and directly sequenced using the Kan3 or RB3 primer. The site and orientation of the T-DNA insertion was identified by use of the BLAST alignment search tool (*12*) and the TAIR database. Sites of the T-DNA element insertions are provided in Table S2. Immunoblot analysis of sucrose gradient fractionated polysomes was used to confirm that the established lines accumulate FLAG-RPL18 in both small and large polysome complexes.

Fluorescence Confocal Microscopy. *p:FLAG-GFP-RPL18* transgenics were produced to verify the cell-type specific expression of each promoter. Seven-d-old kanamycin resistant T1 seedlings were evaluated for GFP fluorescence under a stereo-microscope (Leica MZ FL III; Leica Microsystems). At least 50 individual plants per promoter were observed. The location of GFP fluorescence was consistent for each promoter, although the intensity of fluorescence was variable. Since different independent lines were used, differences in the intensity of fluorescence might be due to different context of T-DNA insertion. T1 and T2 seedlings from four to eight individual lines were analyzed by confocal microscopy (Zeiss LSM 510; Carl Zeiss). Samples were excited with 488 nm (Argon Ion Laser), and fluorescence was detected (GFP filter: BP 500-550 IR; chlorophyll filter: LP 650). For the analysis of T2 seedlings, roots were briefly stained with 10 μg mL^{-1} propidium iodide and cell walls were visualized by use of the chlorophyll-specific settings.

Growth of Seedlings on Solid Medium and Oxygen Deprivation. Seeds were surface sterilized by incubation for 5 min in 95 % (v/v) ethanol followed by 10 min in 20 % (v/v) bleach with 0.1 % (v/v) Tween-20, rinsed in sterile water, and imbibed at 4 °C for 3 d. Seeds were transferred to plates with solid MS media [0.43 % (w/v) Murashigi Skoog (MS)

salts (Sigma)], 0.4 % (w/v) phytagel (Sigma), 1 % (w/v) sucrose, pH 5.7), and placed at a vertical orientation in a growth chamber (Percival Scientific, Inc., model CU36L5C8) under long day conditions (16 h light at ~80 μmol photons m^{-2} s^{-1}/ 8 h darkness) at 23 °C. After 7 d, stress treatments were commenced after the end of the 16-h-day. Oxygen deprivation (hypoxia stress, HS) was imposed exactly as described by Branco-Price et al. (*6*). Briefly, plates were placed vertically in Lucite chambers into which 99.998 % (v/v) argon gas was pumped and allowed to exit under positive pressure. The time required to purge the chambers of air was about 1.5 h. This treatment deprives the plants of oxygen and carbon dioxide, thereby limiting both photosynthesis and aerobic respiration. For non-stress (NS) treatment, plates were placed in identical chambers open to ambient air. Both treatments were carried out under dim light (5 to 7 μmol photons m^{-2} s^{-1}) at room temperature (23 to 25 °C). After 2 h of treatment tissues were harvested into liquid N_2, pulverized, and stored at – 80 °C. For one experiment set, the apical 1 cm of the root was harvested. For another experiment set, the root below the hypocotyl-root junction and the shoot were separately collected. Tissue harvest was accomplished within 3 min of removal from the treatment chamber.

Measurement of Seedling ATP Content. The *p35S:FLAG-RPL18* line was used to extract and analyze metabolite contents from roots and shoots of Arabidopsis plants after 2 h hypoxia. Five biological replicate samples were used to quantify ATP content as described in ref. *13*.

Quantitative Assessment of Polysomes. Polysomes were obtained from extracts of seedling organs by pelleting through a sucrose cushion, further fractionation over sucrose

density gradients and quantified exactly as described by Branco-Price et al. (*5*). Four biological replicates were analyzed.

Immunopurification of Ribosomes. The immunopurification of ribosomes from *p:FLAG-RPL18* lines (individual 60S subunits, ribosomes and polysomes) was accomplished as described previously (*6, 8*) and further detailed in Mustroph et al. (*14*). Briefly, frozen tissue was homogenized in Polysome Extraction Buffer (PEB; 200 mM Tris-HCl, pH 9.0, 200 mM KCl, 25 mM ethylene glycol tetraacetic acid (EGTA), 36 mM $MgCl_2$, 1% (v/v) octylphenyl-polyethylene glycol (Igepal CA-630), 1% (v/v) polyoxyethylene(23) lauryl ether (Brig 35), 1% (v/v) Triton X-100, 1% (v/v) Tween-20, 1% (v/v) polyoxyethylene 10 tridecyl ether, 1% (v/v) sodium deoxycholate, 1 mM dithiothreitol (DTT), 50 µg mL^{-1} cycloheximide, 50 µg mL^{-1} chloramphenicol, 0.5 mg mL^{-1} heparin) using 2.5 mL PEB per mL tissue. A typical extraction was 2 to 3 ml packed volume of frozen pulverised root or root tip tissue or 4 to 6 mL shoot tissue. Homogenates were clarified by centrifugation at 16,000 *g* for 15 min and filtrated with cheesecloth. An aliquot of 600 µL of the supernatant was reserved for isolation of total RNA. To the remaining supernatant 150 µL of EZ-View anti-FLAG agarose beads (Sigma) were added and incubated at 4 °C for 2 h with gentle shaking. The beads were recovered by centrifugation at 3,500 *g*, and washed four times for 5 min each with 6 mL of wash buffer (200 mM Tris-HCl, pH 9.0, 200 mM KCl, 25 mM EGTA, 36 mM $MgCl_2$, 5 mM DTT, 50 µg mL^{-1} cycloheximide, 50 µg mL^{-1} chloramphenicol). Polysomes were eluted by resuspension of the washed beads in 300 µL of wash buffer per 100 µl beads that additionally contained 20 U mL^{-1} of RNase inhibitor (Promega) and 200 µg mL^{-1} of $[FLAG]_3$ peptide (Sigma) at 4 °C for 30 min.

RNA extraction was performed by addition of two volumes of 8 M guanidine-HCl and three volumes of ethanol to the cleared eluate, incubation overnight at –20 °C and pelleting by centrifugation at 15,000 *g* for 45 min. RNA samples were further purified using RNeasy columns (Qiagen) as described previously (*6*). The yield of RNA obtained by immunoprecipitation of ribosome complexes varied in the different *p:FLAG-RPL18* lines, from 1 ng per mL tissue for *pKAT:FLAG-RPL18* to 1 μg per mL tissue for *p35S:FLAG-RPL18*. Total RNA was extracted in the same manner from the reserved cell lysate.

RNA Quantitation, cDNA Amplification and DNA Microarray Hybridizations. Total and immunopurified RNA yields were quantified by use of a NanoDrop ND-1000 UV-Vis Spectrophotometer according to the manufacture's instructions (Nanodrop Technology). RNA quality was assessed using an Agilent 2100 Bioanalyzer with either RNA 6000 Nano or Pico Assay reagent kits (Agilent Technology). Only samples with no signs of rRNA degradation were used to generate probes. For the root-tip mRNA samples, hybridization probe preparation included two linear rounds of target amplification from 400 pg of total or immunopurified RNA using the TargetAmp 2-Round Aminoallyl aRNA Amplification kit 1.0 according to the manufacturer's instructions (Epicenter Biotechnologies). The biotinylated aRNA was purified by use of an RNeasy spin column (Qiagen), quantified by detection of A_{260}/A_{280} with the Nanodrop spectrophotometer and further evaluated with the Agilent Bioanalyzer. For the whole root and shoot mRNA samples, hybridization probe preparation included a two-step-amplification from 15 to 100 ng RNA by use of the Affymetrix protocol. Biotin-labeled cRNA was synthesized using the GeneChip IVT Labeling Kit (Affymetrix). Hybridizations against Arabidopsis ATH1 Genome Array (GeneChip System; Affymetrix) chips were performed at 45 °C for 16 h, in a rotating

platform, using 12 µg of biotin-labeled cRNA. Hybridizations were performed by the Institute for Integrated Genome Biology Core Facility, University of California, Riverside.

Expression Data Analyses. CEL files from the Affymetrix Chips were processed by use of the R program and Bioconductor packages (*15*). The Robust Multi-chip Average (RMA) normalization was performed using the default settings of the corresponding R function (*16*), together with previously published CEL files from a closely related experiment (*6*) (Dataset S1, sheet *d*). To estimate the amount of expressed mRNA, the present call information of the non-parametric Wilcoxon signed rank test (PMA values, *17*) was computed with the "affy" package (*18*) (Dataset S1, sheet *a*). Hybridization data from at least two biological replicates were generated for each *p:FLAG-RPL18* line, tissue sample and treatment. The degree of correlation between hybridizations of biological replicate samples was generated from the RMA normalized signal values (R^2 values, Dataset S1, sheet *g*). RMA-normalized samples were hierarchically clustered by the R-function HCLUST using complete linkage as the cluster joining method and Pearson correlation coefficients as similarity measure (Fig. S14).

The ATH1 Genome Array microarray platform that was utilized for this study is available at the GEO (Gene Expression Omnibus) data repository under accession number GPL198. The microarray experiments reported here are described following MIAME guidelines and deposited in GEO under the accession numbers GSE14493 and GSE14502 in the superSeries GSE14578.

Differential Gene Expression Analysis of Cell-Type Specific Genes. Analysis of

differentially expressed genes (DEGs) was performed with the LIMMA package using the RMA normalized expression values (*19*). The Benjamini and Hochberg method was selected to adjust P-values for multiple testing and to determine false discovery rates (FDRs) (*20*). As confidence threshold, an FDR of <0.01 was used.

To identify mRNAs enriched in specific cell types, the following systematic comparisons were performed: immunopurified RNA of control or hypoxia stressed samples were compared to all other non-overlapping cell types in the same organ and under the same treatment conditions. The complete list of comparisons is provided in Dataset S2, sheet *a*. Genes were deemed as significantly enriched or depleted in a specific cell type (mRNA population) if the following criteria were met: >2-fold change and FDR <0.01 for each pairwise comparison. Subsequently, the overlap of the significantly enriched or depleted gene lists for each cell type was recorded (Dataset S2, sheet *a*). In addition to the gene lists, the mean of the signal-log-ratios (SLRs) and the FDRs of utilized comparisons for each cell type were calculated (Dataset S2, sheet *a*). Because of partial overlap in expression of some promoters in certain cell types (for example stele: *pSHR* and *pWOL* mRNA populations partially overlap with *pSUC* and *pSultr2;2* mRNA populations; epidermis: *pKAT, pGL2* and *pCER5* mRNA populations partially overlap with each other), two comparison stringencies were used for root stele and most shoot samples.

For the comparison of the mRNAs enriched in specific cell types with published microarray data, publicly available CEL files (*21-25*) were analyzed using the pipeline described above. The RMA normalization step was always applied to samples published as one experiment. The LIMMA DEG analysis was performed as a comparison of each specific shoot cell type against the corresponding control dataset (*21-24*), or with the queries described in Dataset S4, sheet *c* in the style of the analysis of our own data (*25*).

Comparisons of overlap between published data and our data are found in Datasets S2 and S4.

Identification of Co-Expression Patterns Across Cell Types and Organs by Fuzzy k-Means Clustering. Data were analyzed by fuzzy k-means clustering with the fanny function from the cluster package in R. For this analysis, the means of biological replicates of RMA-normalized data were used. Genes were removed from the dataset if they encoded mitochondrial or plastid transcripts, or if they were not called as present by MAS5 in any sample pair (P in all replicates of one sample type, across organs, cell types and stress treatments). Furthermore, data were filtered prior to clustering by removing any genes that did not show at least a 2-fold difference over the mean across all measurements. This filtering retained 11,273 of the 17,468 present genes. The settings for the FANNY algorithm were the following: distance measure = (1 - Pearson correlation), number of clusters = 60, membership exponent = 1.1, maximal number of iterations = 5000, according to Brady et al. (*25*). Preliminary runs established that the membership exponent and cluster number were in the appropriate range for the dataset. Following the clustering the groups were reduced from 60 to 59 clusters by collapsing with a Pearson correlation coefficient larger of 0.95 as described previously (*25, 26*). The fuzzy algorithm was applied for the whole control treatment (non-stress) dataset and independently for the hypoxia treatment dataset, to avoid disturbing influences of the stress treatment on the cluster formation. After fuzzy clustering, the median expression values of the clusters were calculated as described previously (*25, 26*). For this, all genes with a cluster coefficient >0.4 were assigned to the corresponding cluster. Because the coefficient can take values from 0 to 1 for each cluster

assignment and sums to 1 across all clusters, this setting allowed each gene to be part of a maximum of 2 clusters. For easier visualization, the RMA values were transformed before median calculation by the scale function in the R package "base". The control dataset resulted in 59 final clusters. Final gene-to-cluster assignments are given in Dataset S3. Expression medians and clusters were visualized with the TIGR MEV program.

Differential Expression Analysis of Hypoxia-Induced Genes. RMA-normalized expression data from immunopurified RNA from a cell-specific promoter line under hypoxia was compared with the same line under control conditions by use of Limma (Dataset S5). Criteria for the selection of significantly induced or reduced genes due to the stress were the same as described for the cell-type comparison. The overlap of genes that were significantly induced or reduced in all cell types of one organ was recorded as the "core response". Several approaches were used to identify mRNAs with a different response to hypoxia in specific cell types.

To find general patterns of response to hypoxia, fuzzy k-means clustering was performed with all genes that showed differential expression due to hypoxia as determined by the Limma analysis described above. As for the cell-type fuzzy clustering, RMA normalized mean values were used, but control and hypoxia datasets were combined. The settings for the FANNY algorithm and the cluster post-processing were the same as above, with the exception that the number of clusters was 100 instead of 60. The final gene-to-cluster assignments are given in Dataset S6.

Both analyses described above revealed that many hypoxia-induced mRNAs were induced in all cell types examined, whereas the hypoxia-reduced mRNAs were more cell type specific. To recognize cell-types distinctions in hypoxia response, all mRNAs that

were enriched in a specific cell-type under control conditions (Dataset S2) AND displayed significantly lower expression under hypoxia in that cell type were tabulated (Dataset S3). Those gene lists demonstrate the loss of cell specific gene expression during hypoxic stress.

To identify mRNAs that showed a significantly different response to hypoxia in a specific cell-type as compared to other non-overlapping cell types, DEG analysis was used to compare the SLR of hypoxia versus control for one cell type to the SLR between hypoxia and control of other non-overlapping cell types. The formula for the contrast matrix was: (H_CT1-C_CT1)-(H_CT2-C_CT2), where CT is cell type. Dataset S7 records the comparisons used and the overlap of gene lists for all comparisons.

GO Analyses. The specific gene lists obtained by the Limma and fuzzy k-mean clustering analyses were evaluated for enrichment of genes with specific biological function, molecular process or subcellular component annotations. Enrichment analyses of Gene Ontology (GO) terms were performed as described in Horan et al. (*27*). In summary, the Arabidopsis gene-to-GO mappings from TAIR (available at http://geneontology.org; downloaded June 25, 2008) were used for these analyses. The hypergeometric distribution was applied to test gene sets for the overrepresentation of GO terms. To perform this test, the GOHyperGAll function was used (see refs. *27* and *28*), which computes for a given sample population of genes the enrichment test for all nodes in the GO network, and returns raw and adjusted p-values. As an adjustment method for multiple testing, it uses the Bonferroni method according to Boyle et al. (*29*). GO categories with an adjusted P-value <0.05 were deemed significantly enriched. To remove nested GO terms, we enabled the "simplify" step of the GOHyperGAll function. GO enrichment lists can be found in

Datasets S2, S3, S5, S6, and S7. Because of the nature of the P-value calculations, clusters or gene lists with <10 members were not analyzed.

Members of transcription factor families were obtained from TAIR (available at www.arabidopsis.org; accessed October 2, 2008) and AGRIS (*30*). The exact TF family to gene assignment is included in Dataset S2, sheet *a*. The TF family enrichment of gene lists and clusters was calculated with the GOHyperGAll function. The results of this analysis can be found in Datasets S2, S3, S5, S6, and S7. Enrichment of binding sites for transcription factors was determined for specific gene lists for the –1,000 bp promoter region by use of the online tool Athena with the default settings.

1. Masucci JD, et al. (1996) The homeobox gene GLABRA2 is required for position-dependent cell differentiation in the root epidermis of *Arabidopsis thaliana*. *Dev* 122:1253-1260.

2. Szymanski DB, Jilk RA, Pollock SM, Marks MD (1998) Control of GL2 expression in Arabidopsis leaves and trichomes. *Dev* 125:1161-1171.

3. Takahashi H, et al. (2000) The roles of three functional sulphate transporters involved in uptake and translocation of sulphate in *Arabidopsis thaliana*. *Plant J* 23:171-182.

4. Kawaguchi R, Bailey-Serres J (2005) mRNA sequence features that contribute to translational regulation in Arabidopsis. *Nuc Acids Res* 33:955-965.

5. Branco-Price C, Kawaguchi R, Ferriera R, Bailey-Serres J (2005) Genome-wide analysis of transcript abundance and translation in Arabidopsis seedlings subjected to oxygen deprivation. *Ann Bot* 96:647-660.

6. Branco-Price C, Kaiser KA, Jang CJ, Larive CK, Bailey-Serres J (2008) Selective mRNA translation coordinates energetic and metabolic adjustments to cellular oxygen deprivation and reoxygenation in *Arabidopsis thaliana*. *Plant J* 56:743-755.

7. Hajdukiewicz P, Svab Z, Maliga P (1994) The small, versatile pPZP family of Agrobacterium binary vectors for plant transformation. *Plant Mol Biol* 25:989-994.

8. Zanetti ME, Chang I-F, Gong F-C, Galbraith DW, Bailey-Serres J (2005) Immuno-affinity purification of polyribosomal complexes of Arabidopsis for global analysis of gene expression. *Plant Physiol* 138:624-635.

9. Chiu W, et al. (1996) Engineered GFP as a vital reporter in plants. *Current Biol* 6:325-330.

10. Clough SJ, Bent AF (1998) Floral dip: a simplified method for Agrobacterium-mediated transformation of *Arabidopsis thaliana*. *Plant J* 16:735-743.

11. Liu YG, Mitsukawa N, Oosumi T, Whittier RF (1995) Efficient isolation and mapping of Arabidopsis thaliana T-DNA insert junctions by thermal asymmetric interlaced PCR. *Plant J* 8:457-463.

12. Altschul SF, Gish W, Miller W, Myers EW, Lipman DJ (1990) Basic local alignment search tool. *J Mol Biol* 215:403-410.

13. Mustroph A, et al. (2006) Organ-specific analysis of the anaerobic primary metabolism in rice and wheat seedlings. I: Dark ethanol production is dominated by the shoots. *Planta* 225:103-114.

14. Mustroph A, Juntawong P, Bailey-Serres J (2009) Isolation of plant polysomal mRNA by differential centrifugation and ribosome immunopurification methods. *Methods in Molecular Biology: Plant Systems Biology,* in press.

15. Gentleman R, et al. (2004) Bioconductor: Open software development for computational biology and bioinformatics. *Genome Biol* 5:R80.

16. Irizarry RA, et al. (2003) Summaries of Affymetrix GeneChip probe level data. *Nucleic Acids Res* 31:e15.

17. Liu WM, et al. (2002) Analysis of high density expression microarrays with signed-rank call algorithms. *Bioinformatics* 18:1593-1599.

18. Gautier L, Cope L, Bolstad BM, Irizarry RA (2004) Affy--analysis of Affymetrix GeneChip data at the probe level. *Bioinformatics* 20:307-315.

19. Smyth GK (2004) Linear models and empirical bayes methods for assessing differential expression in microarray experiments. *Stat Appl Genet Mol Biol* 3:Article3.

20. Benjamini Y, Hochberg Y (1995) Controlling the false discovery rate: a practical and powerful approach to multiple testing. *J Roy Statist Soc B* 57:289-300.

21. Suh MC, et al. (2005) Cuticular lipid composition, surface structure, and gene expression in Arabidopsis stem epidermis. *Plant Physiol* 139:1649-1665.

22. Yang Y, Costa A, Leonhardt N, Siegel RS, Schroeder JI (2008) Isolation of a strong Arabidopsis guard cell promoter and its potential as a research tool. *Plant Methods* 4:6.

23. Jakoby MJ, et al. (2008) Transcriptional profiling of mature Arabidopsis trichomes reveals that NOECK encodes the MIXTA-like transcriptional regulator MYB106. *Plant Physiol* 148:1583-1602.

24. Zhao C, Craig JC, Petzold HE, Dickerman AW, Beers EP (2005) The xylem and phloem transcriptomes from secondary tissues of the Arabidopsis root-hypocotyl. *Plant Physiol* 138:803-818.

25. Brady SM, et al. (2007) A high-resolution root spatiotemporal map reveals dominant expression patterns. *Science* 318:801-806.

26. Orlando DA, Brady SM, Koch JD, Dinneny JR, Benfey PN (2009) Manipulating large scale Arabidopsis microarray expression data: Identifying dominant expression patterns and biological process enrichment. *Methods in Molecular Biology: Plant Systems Biology*, in press.

27. Horan K, et al. (2008) Annotating genes of known and unknown function by large-scale coexpression analysis. *Plant Physiol* 147:41-57.

28. Falcon S, Gentleman R (2007) Using GOstats to test gene lists for GO term association. *Bioinformatics* 23:257–258.

29. Boyle EI, et al. (2004) GO::TermFinder--Open source software for accessing Gene Ontology information and finding significantly enriched Gene Ontology terms associated with a list of genes. *Bioinformatics* 20:3710-3715.

30. Davuluri RV, et al. (2003) AGRIS: Arabidopsis Gene Regulatory Information Server. An information resource of Arabidopsis cis-regulatory elements and transcription factors. *BMC Bioinformatics* 4:25. Available at http://arabidopsis.med.ohio-state.edu. Accessed October 2, 2008.

31. Wysocka-Diller JW, Helariutta Y, Fukaki H, Malamy JE, Benfey PN (2000) Molecular analysis of SCARECROW function reveals a radial patterning mechanism common to root and shoot. *Dev* 127:595-603.

32. Helariutta Y, et al. (2000) The SHORT-ROOT gene controls radial patterning of the Arabidopsis root through radial signaling. *Cell* 101:555-567.

33. Estelle M (2001) Cytokinin receptor: Just another histidine kinase. *Curr Biol* 11:271-273.

34. Heidstra R, Welch D, Scheres B (2004) Mosaic analyses using marked activation and deletion clones dissect Arabidopsis SCARECROW action in asymmetric cell division. *Genes & Dev* 18:1964-1969.

35. Mace DL, et al. (2006) Quantification of transcription factor expression from Arabidopsis images. *Bioinformatics* 22:e323-e331.

36. Williams ME, Sussex IM (1995) Developmental regulation of ribosomal protein L16 genes in Arabidopsis thaliana. *Plant J* 8:65-76.

37. Imlau A, Truernit E, Sauer N (1999) Cell-to-cell and long-distance trafficking of the green fluorescent protein in the phloem and symplastic unloading of the protein into sink tissues. *Plant Cell* 11:309-322.

38. Pighin JA, et al. (2004) Plant cuticular lipid export requires an ABC transporter. *Science* 306:702-704.

39. Nakamura RL, et al. (1995) Expression of an Arabidopsis potassium channel gene in guard cells. *Plant Physiol* 109:371-374.

40. Donald RG, Cashmore AR (1990) Mutation of either G box or I box sequences profoundly affects expression from the Arabidopsis rbcS-1A promoter. *EMBO J* 9:1717-1726.

41. Scharf KD, Siddique M, Vierling E (2001) The expanding family of *Arabidopsis thaliana* small heat stress proteins and a new family of proteins containing alpha-crystallin domains (Acd proteins). *Cell Stress Chaperones* 6:225-237.

42. Nakano T, Suzuki K, Fujimura T, Shinshi H (2006) Genome-wide analysis of the ERF gene family in Arabidopsis and rice. *Plant Physiol* 140:411-432.

SI Methods Fig. S1. T-DNA insertions used in this study. Maps include GATA site for promoter insertion and selected restriction sites. (*A*) *p35S:HF-RPL18*; (*B*) *pGATA:HF-RPL18*; (*C*) *pGATA:HF-GFP-RPL18*. HF = His-FLAG-tag; OCS = OCS terminator; NPTII = Kanamycin resistance gene; LB = left border of T-DNA; RB = right border of T-DNA; 35Sm, 820 nt CaMV 35S promoter; numbers: estimated nucleotide lengths of DNA sequences. Arrows indicate direction of transcription.

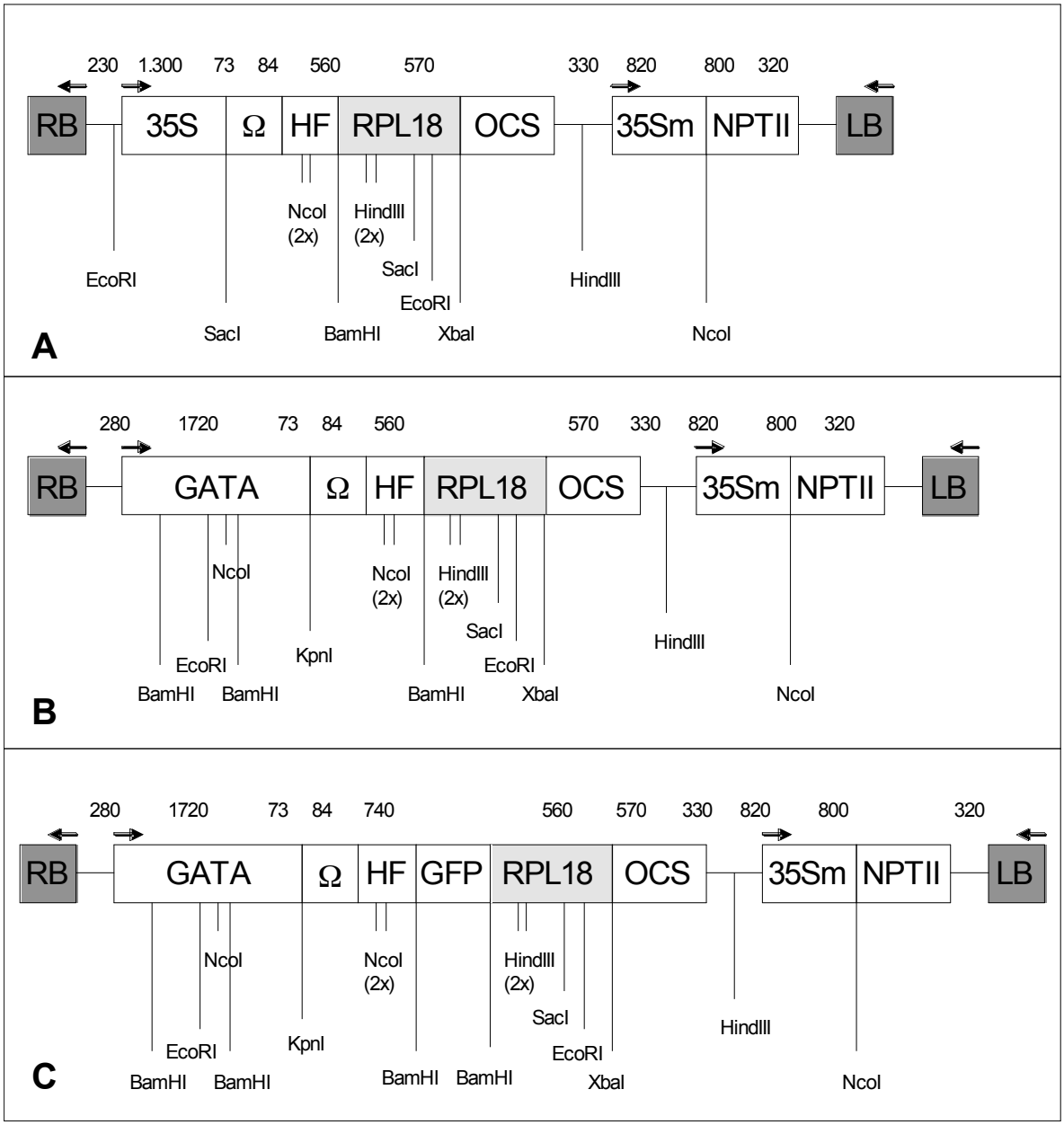

Fig. S1. Representative images demonstrating the specificity of promoter activity in T1 and T2 transgenics produced for each of the cell/region specific promoters. Individual promoters were used to drive the production of FLAG-GFP-RPL18 in transgenic Arabidopsis. Over 50 T1 seedlings (7-d-old) produced from multiple plants were evaluated to confirm that the expression pattern of each promoter was consistent. Promoter activity was re-evaluated in the T2 generation. All of the promoters showed highly consistent expression patterns. Green = GFP fluorescence, red = chlorophyll in shoots, Propidium iodide staining in roots. (Scale bar, 50 μm.) (*A*) Aerial organs. (*B*) Roots. For each row, the following sections of the roots are shown from left to right: root tip region; higher magnification of propidium iodide stained root tip image; root maturation zone, with lateral root primordia; transverse section through elongation zone for selected lines. Transverse sections are optical sections through the intact root by confocal microscopy. (*C*) Roots. For each row, the following sections of the roots are shown from left to right: root maturation zone; higher magnification of propidium iodide stained root maturation zone image; root tip; optical transverse section through root maturation zone. (*D*) Subcellular localization of GFP-tagged ribosomes in a *p35S:FLAG-GFP-RPL18* transgenic. As would be expected for a RP, GFP is localized in the cytoplasm and enriched in the nucleoli (white arrows) as represented by a (*i*) leaf mesophyll cell and (*ii*) root epidermis cell.

Fig. S1A

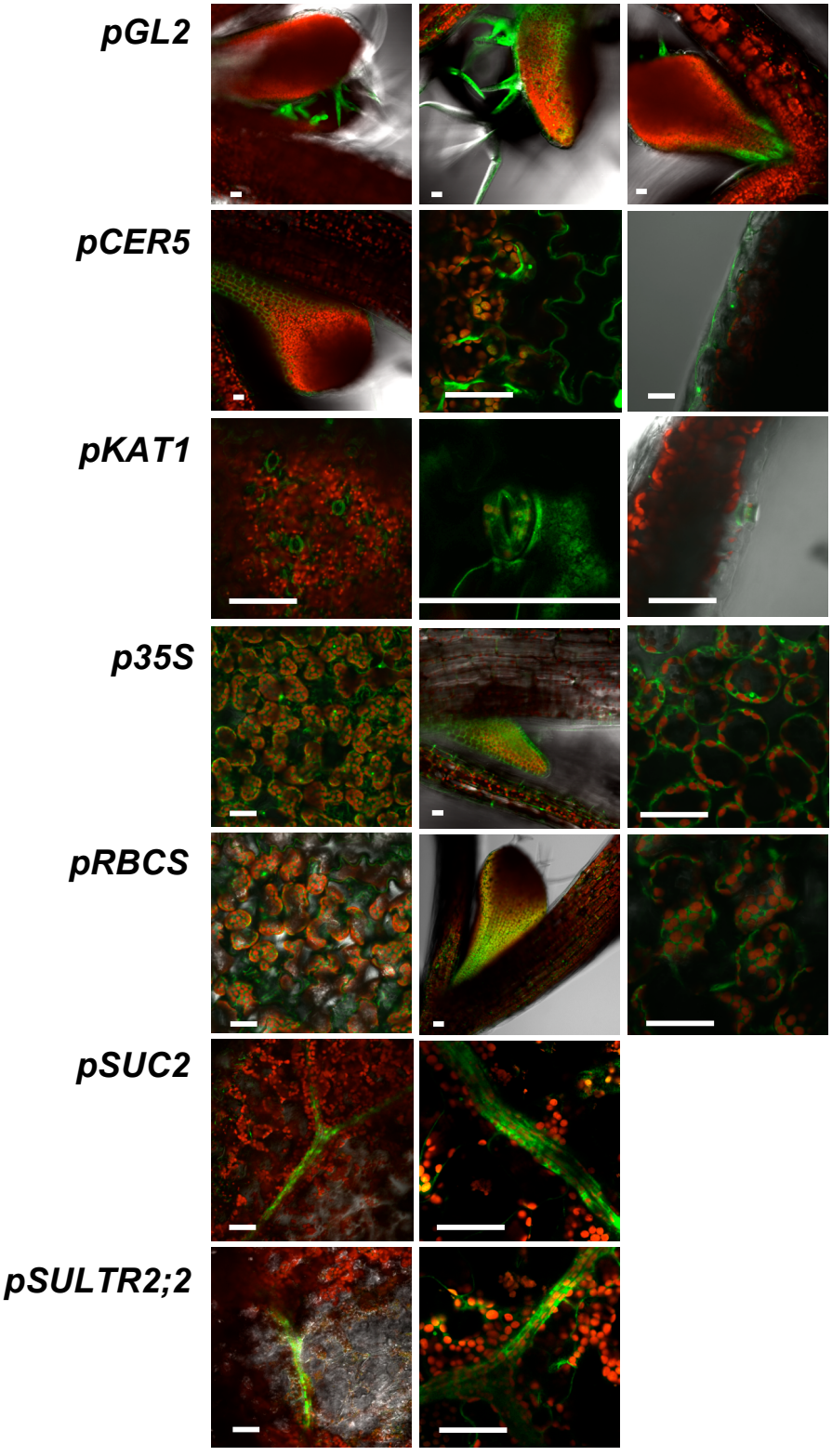

Fig. S1B

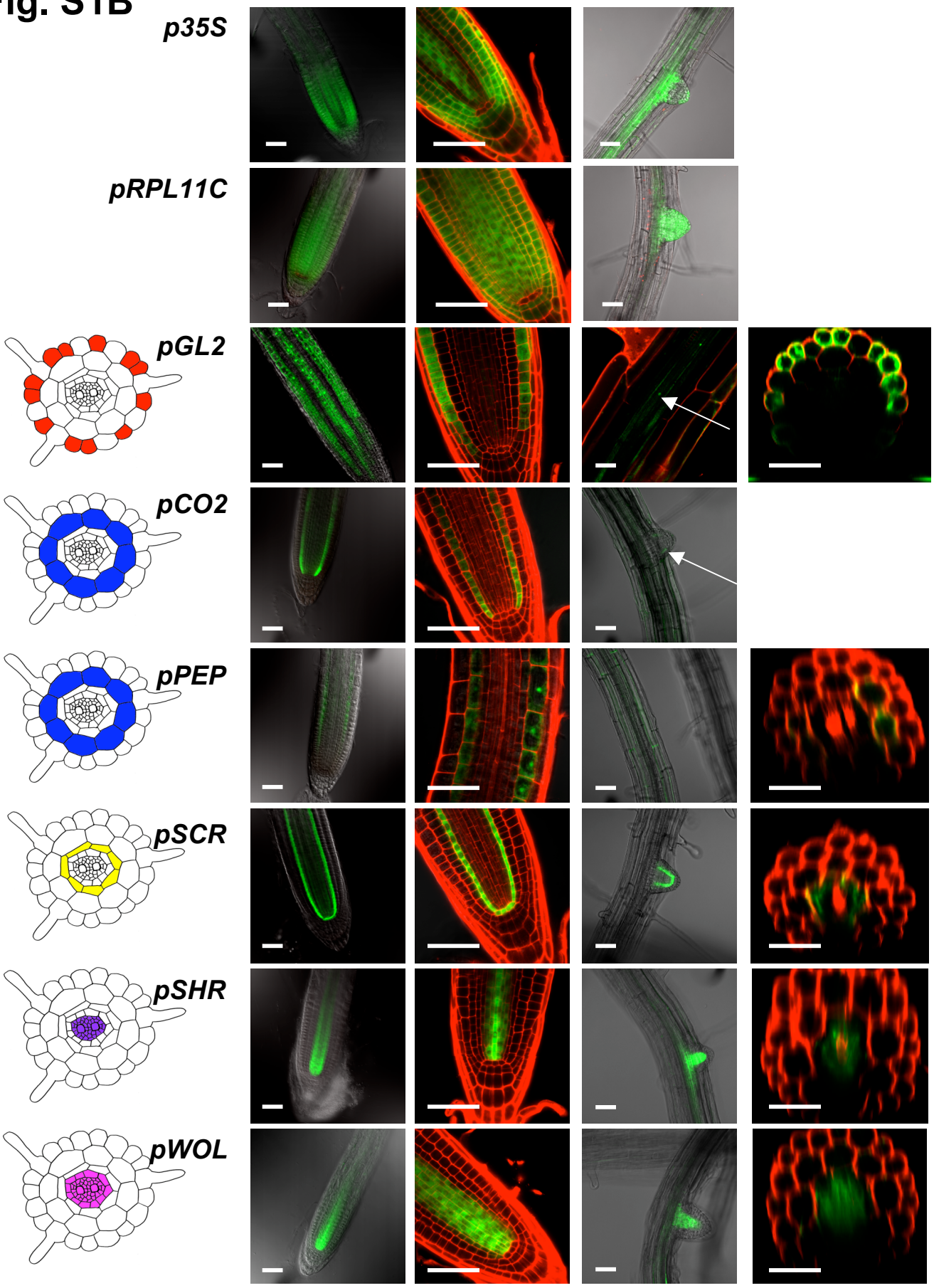

Fig. S1C, D

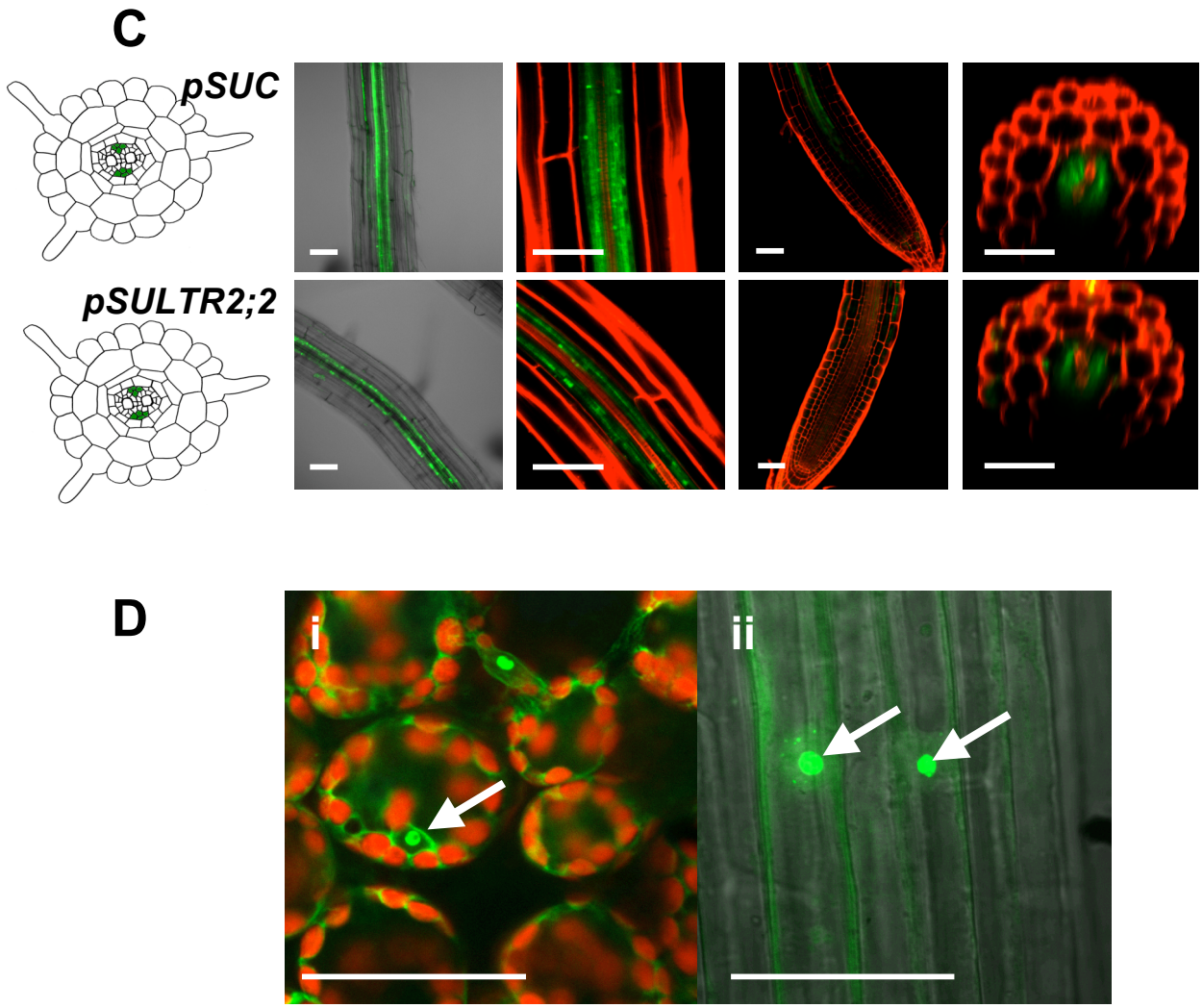

Fig. S2. Immunopurified polysomal mRNA populations obtained from two distinct *pGL2:FLAG-RPL18* transgenic lines are highly correlated. (*A*) Schematic of the insertion site of T-DNA in each transgenic line determined by TAIL-PCR; (*B*) Correlation between probe pair set signal values for polysomal mRNA from 7-d-old seedlings of the two *pGL2:FLAG-RPL18* lines. (*C*) Correlation between probe pair set signal values for polysomal mRNA from 7-d-old seedlings of *pGL2:FLAG-RPL18-1* from two independent biological replicate experiments.

Fig. S2

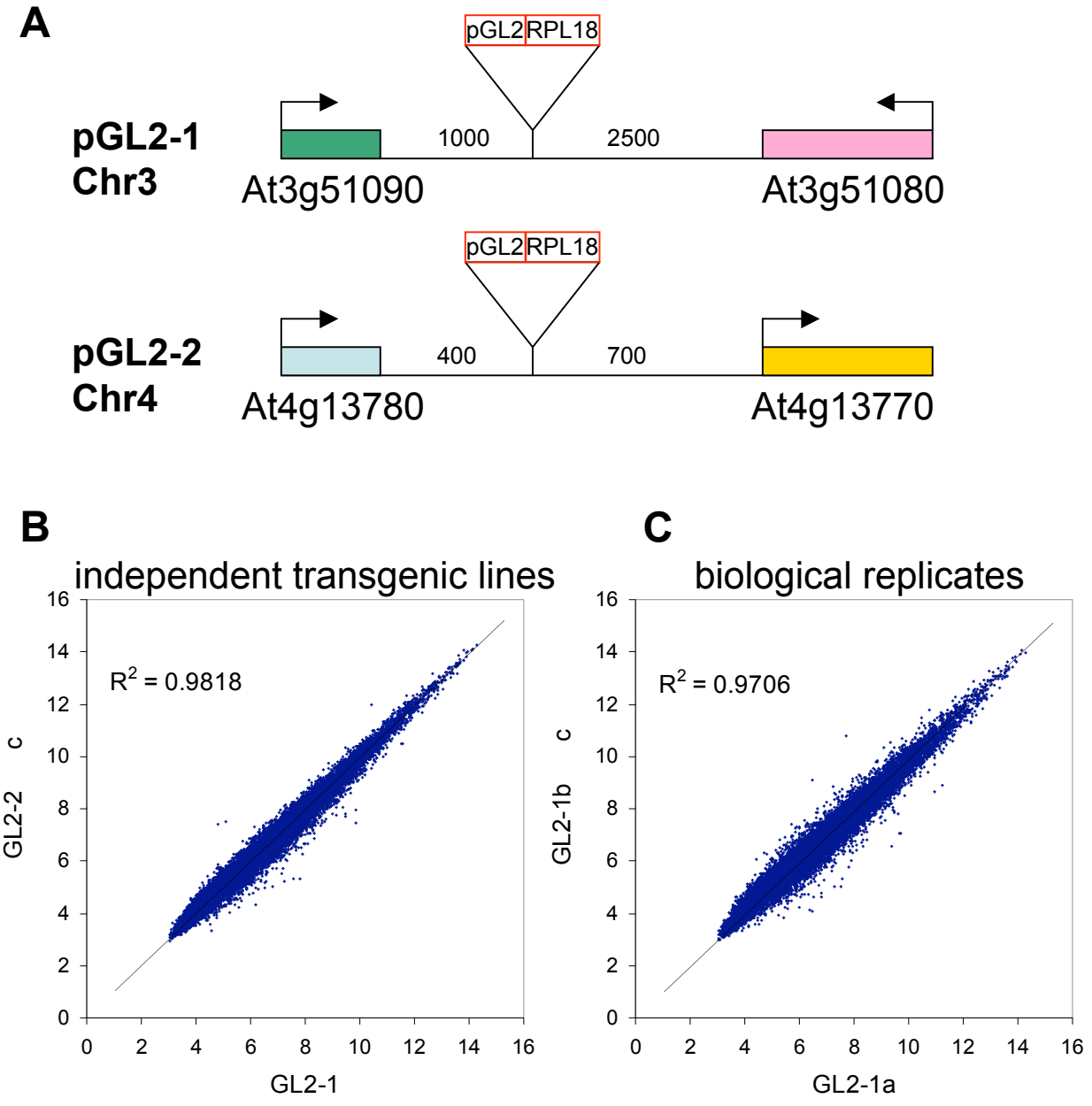
A
pGL2
RPL18
pGL2-1
Chr3
1000
2500
At3g51090
At3g51080
pGL2
RPL18
pGL2-2
Chr4
400
700
At4g13780
At4g13770
B
independent transgenic lines
R2 = 0.9818
GL2-2 c
GL2-1
C
biological replicates
R2 = 0.9706
GL2-1b c
GL2-1a

Fig. S3. Overview of isolation of RNA populations and post-hybridization analyses. Computational analysis of microarray data. *1 – comparisons made: cell type versus subsets of non-overlapping cell types (see Dataset S2 for details) of one organ of control and hypoxic stressed seedlings. *2 – for each cell type, hypoxia was compared to aerated control.

Fig. S3

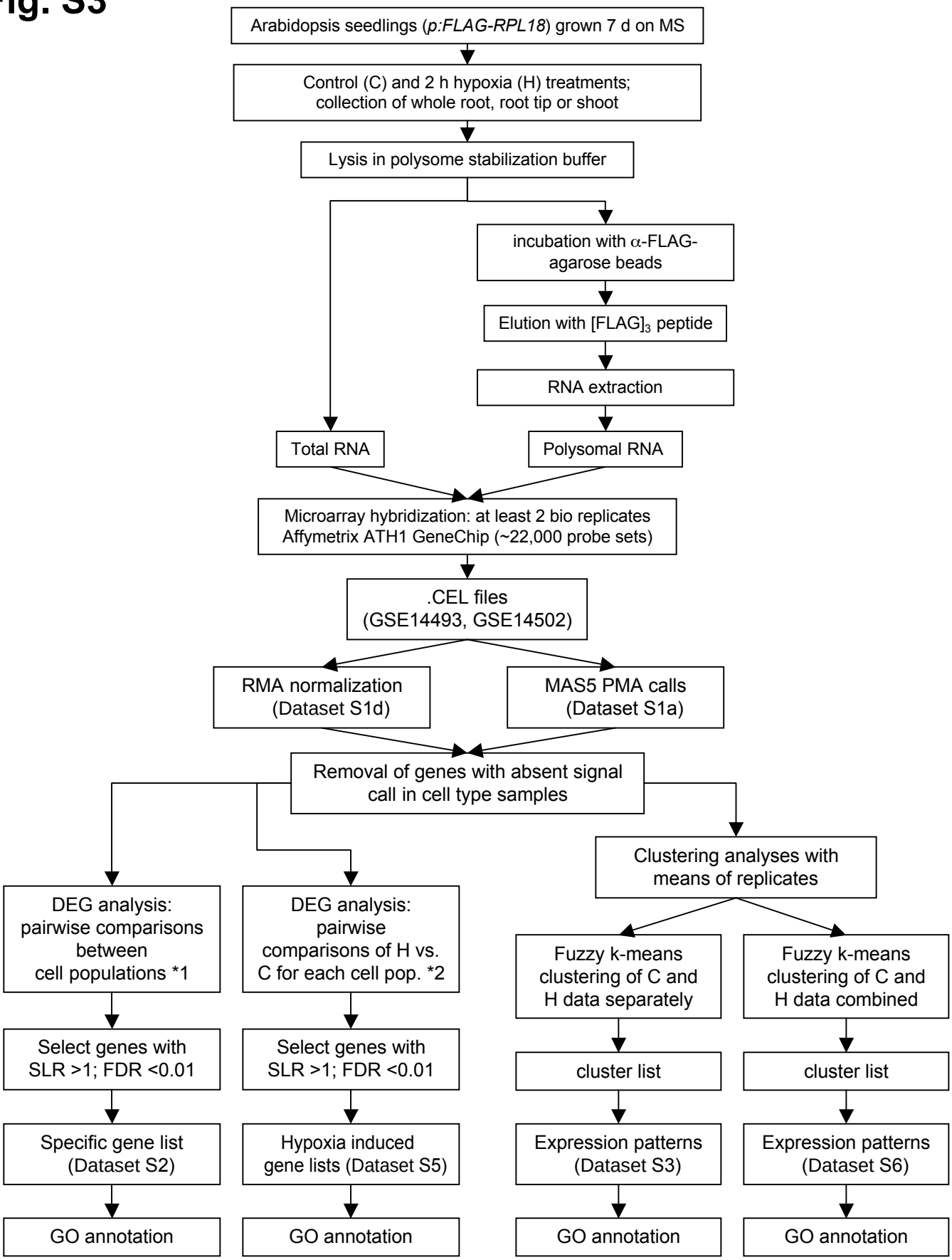
Arabidopsis seedlings (*p:FLAG-RPL18*) grown 7 d on MS
Control (C) and 2 h hypoxia (H) treatments; collection of whole root, root tip or shoot
Lysis in polysome stabilization buffer
incubation with α-FLAG-agarose beads
Elution with [FLAG]3 peptide
RNA extraction
Total RNA
Polysomal RNA
Microarray hybridization: at least 2 bio replicates Affymetrix ATH1 GeneChip (~22,000 probe sets)
.CEL files (GSE14493, GSE14502)
RMA normalization (Dataset S1d)
MAS5 PMA calls (Dataset S1a)
Removal of genes with absent signal call in cell type samples
DEG analysis: pairwise comparisons between cell populations *1
DEG analysis: pairwise comparisons of H vs. C for each cell pop. *2
Clustering analyses with means of replicates
Select genes with SLR >1; FDR <0.01
Select genes with SLR >1; FDR <0.01
Fuzzy k-means clustering of C and H data separately
Fuzzy k-means clustering of C and H data combined
Specific gene list (Dataset S2)
Hypoxia induced gene lists (Dataset S5)
cluster list
cluster list
Expression patterns (Dataset S3)
Expression patterns (Dataset S6)
GO annotation
GO annotation
GO annotation
GO annotation

Fig. S4. Data display available on the eFP browser. Absolute expression values (MAS5 normalized) and SLRs from the differential gene expression analysis (from RMA-normalized data, see Dataset S2, sheet *a*) can be visualized on a gene-by-gene basis using the eFP platform (currently accessible at http://bioinfo.ucr.edu/~cjang/cgi-bin/absolute.cgi for absolute (MAS5) values and at http://bioinfo.ucr.edu/~cjang/cgi-bin/relative.cgi for relative (SLR) values; to be added to the Toronto eFP site). Data are shown for two transcription factors with cell-type specific expression. At3g24140 (FAMA; bHLH TF) and At5g65790 (ATMYB68; MYB TF) are mRNAs that are enriched in guard cells and root endodermis, respectively. Sucrose synthase 1 (*SUS1*, At5g20830) provides an example of an mRNA that is enriched in phloem companion cells under control conditions and hypoxia-induced across cell types. Views in eFP include three comparisons: shoot samples, shoot and whole root samples, or whole root and root tip samples as exemplified in the examples. Left panel, polysomal mRNA transcript abundance from MAS5 normalized raw data (referred to as "Absolute values"). Right panel, SLRs exposing cell-type enrichment by comparison to non-overlapping cell types in the same organ (values from Dataset S2, sheet *a*, referred to as "Relative values").

Fig. S4

mRNA abundance (MAS5 values)

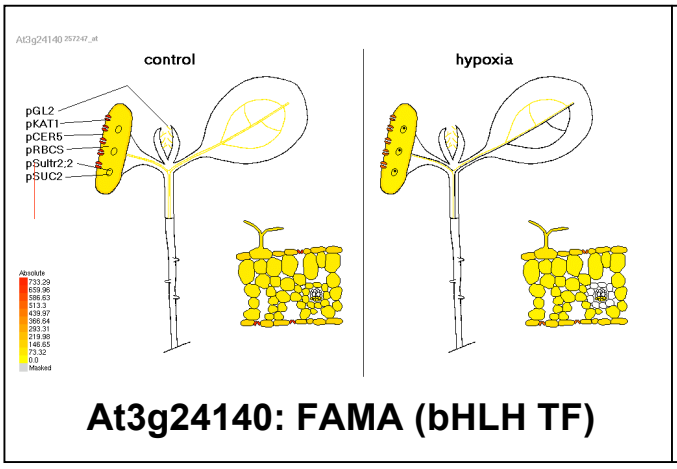

At3g24140: FAMA (bHLH TF)

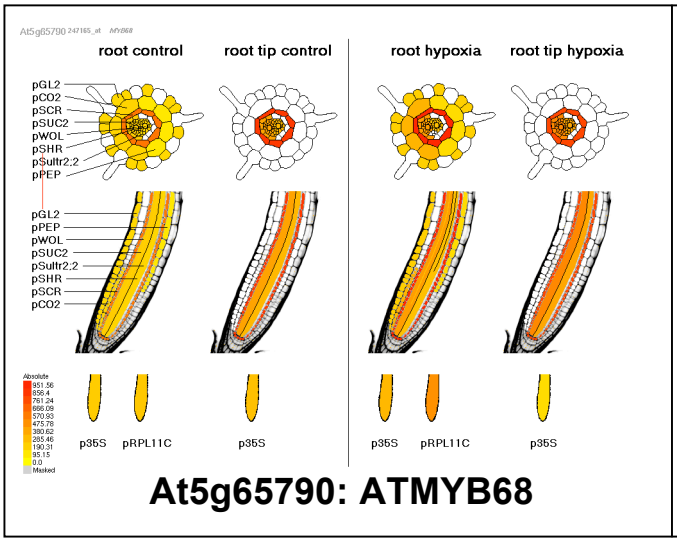

At5g65790: ATMYB68

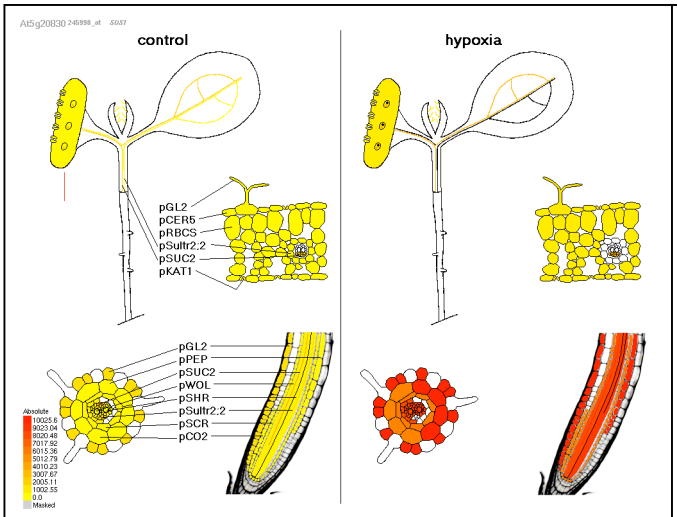

At5g20830: *SUS1*

mRNA enrichment in cell populations (SLR of RMA values)

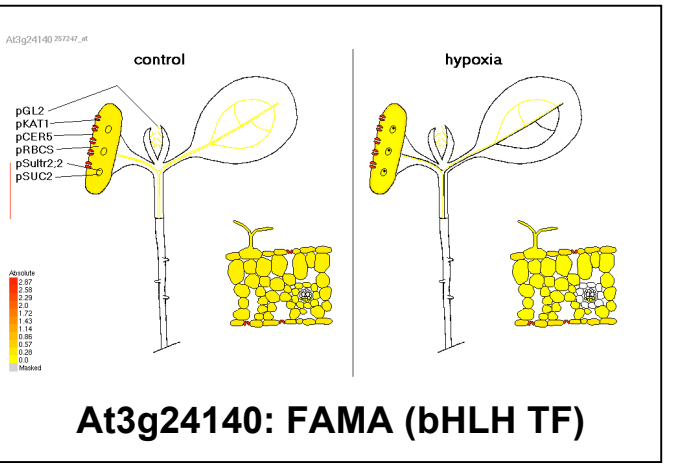

At3g24140: FAMA (bHLH TF)

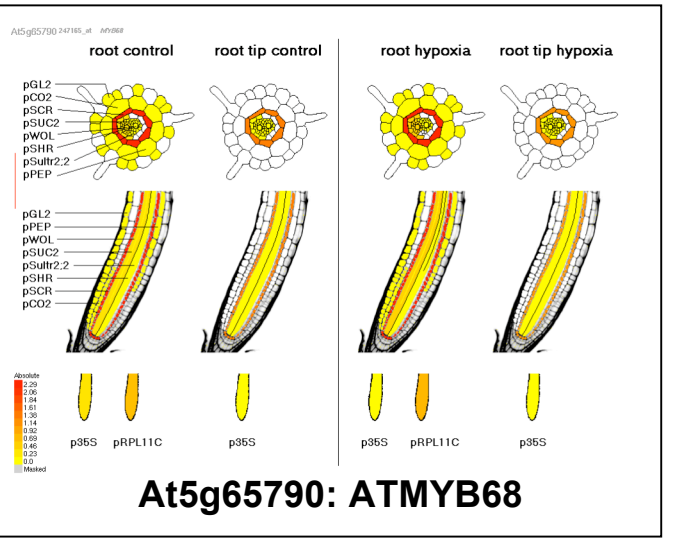

At5g65790: ATMYB68

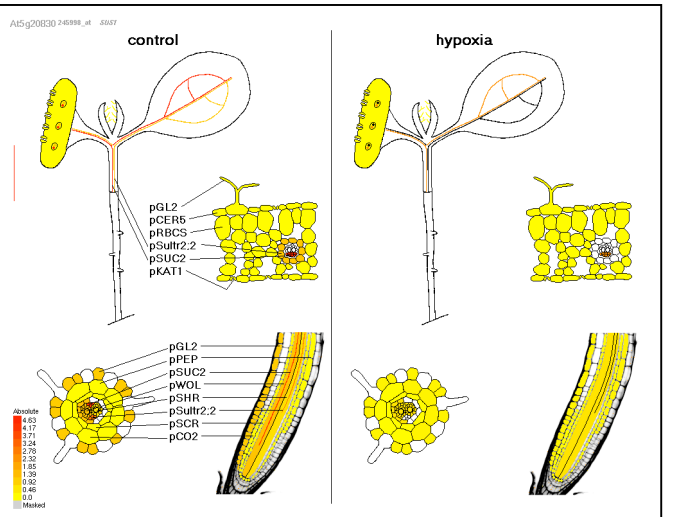

At5g20830: *SUS1*

Fig. S5. Pattern of cell-type specific gene expression across all organs. (*A*) Means of RMA-normalized data of 11,273 genes (probe pair sets) from plants grown under control conditions were analyzed by fuzzy k-means clustering (Expanded Fig. 2). The median expression value of the 59 gene clusters was calculated from scaled values. The clusters were organized to visualize trends in cell-type mRNA enrichment. Each cluster includes a group of genes with similar enrichment/depletion across the samples. Sample names correspond to the promoters used for FLAG-RPL18 expression (Table 1). White bars divide different organs. Blue arrows indicate clusters presented in Fig. 2*A*. Red arrows indicate clusters presented in *B*. (*B*) Examples of clusters with strong cell-type enrichment from *A*. The colored panels show scaled RMA-values for all genes in a cluster; tables list the most significantly enriched Gene Ontology (GO) categories. GO enrichment P-values were calculated by the GOHyperGAll function (*27*). Dataset S3 contains all fuzzy k-means cluster and GO data.

Fig. S5A

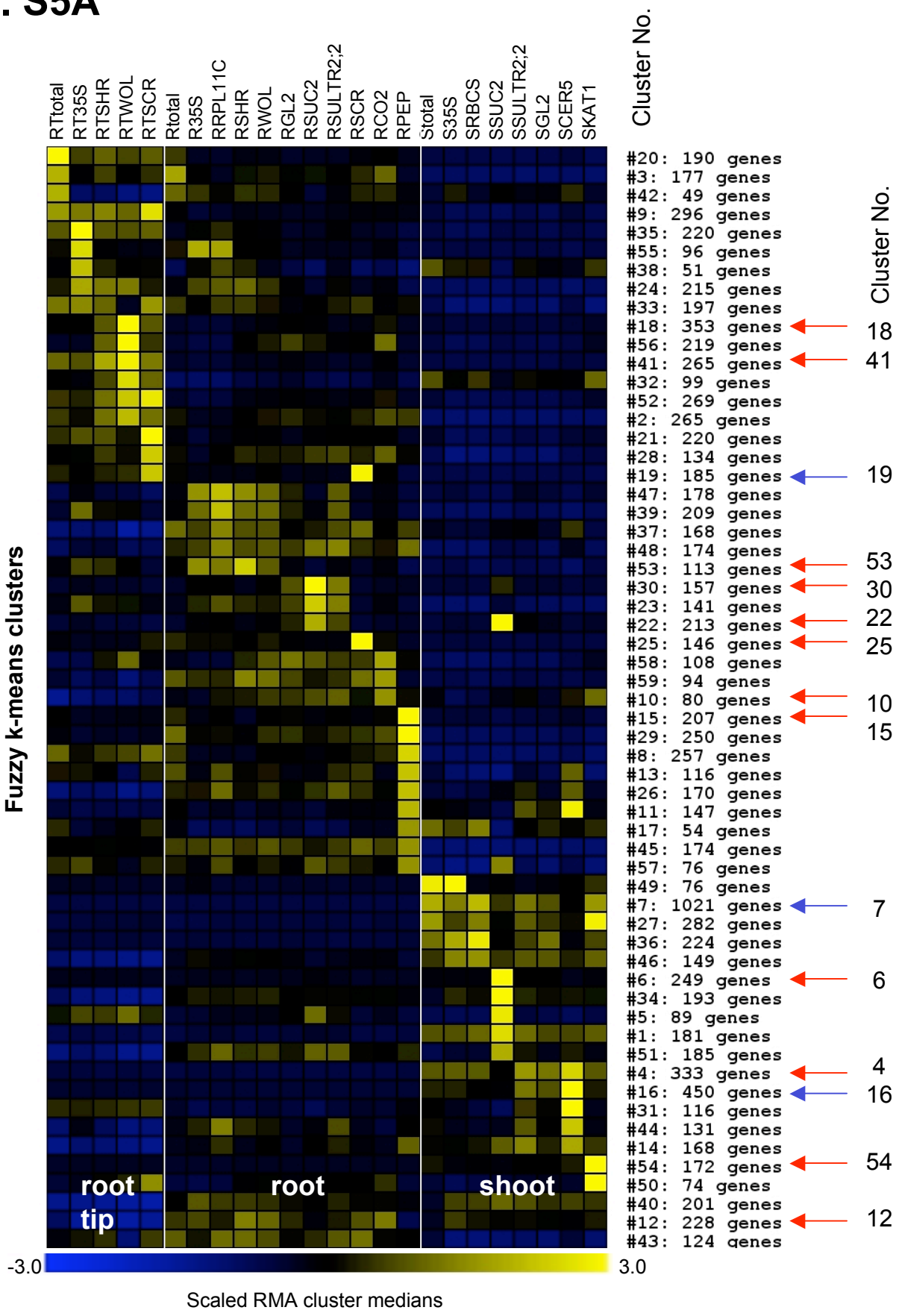
RTtotal
RT35S
RTSHR
RTWOL
RTSCR
Rtotal
R35S
RRPL11C
RSHR
RWOL
RGL2
RSUC2
RSULTR2;2
RSCR
RCO2
RPEP
Stotal
S35S
SRBCS
SSUC2
SSULTR2;2
SGL2
SCER5
SKAT1
Cluster No.
Fuzzy k-means clusters
root tip
root
shoot
#20: 190 genes
#3: 177 genes
#42: 49 genes
#9: 296 genes
#35: 220 genes
#55: 96 genes
#38: 51 genes
#24: 215 genes
#33: 197 genes
#18: 353 genes
#56: 219 genes
#41: 265 genes
#32: 99 genes
#52: 269 genes
#2: 265 genes
#21: 220 genes
#28: 134 genes
#19: 185 genes
#47: 178 genes
#39: 209 genes
#37: 168 genes
#48: 174 genes
#53: 113 genes
#30: 157 genes
#23: 141 genes
#22: 213 genes
#25: 146 genes
#58: 108 genes
#59: 94 genes
#10: 80 genes
#15: 207 genes
#29: 250 genes
#8: 257 genes
#13: 116 genes
#26: 170 genes
#11: 147 genes
#17: 54 genes
#45: 174 genes
#57: 76 genes
#49: 76 genes
#7: 1021 genes
#27: 282 genes
#36: 224 genes
#46: 149 genes
#6: 249 genes
#34: 193 genes
#5: 89 genes
#1: 181 genes
#51: 185 genes
#4: 333 genes
#16: 450 genes
#31: 116 genes
#44: 131 genes
#14: 168 genes
#54: 172 genes
#50: 74 genes
#40: 201 genes
#12: 228 genes
#43: 124 genes
Cluster No.
18
41
19
53
30
22
25
10
15
7
6
4
16
54
12
-3.0
3.0
Scaled RMA cluster medians

Fig. S5B

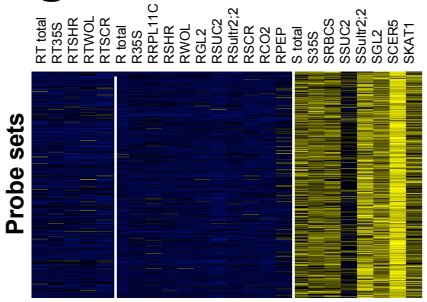

Cluster 4 (epidermis), 333 genes	P(adj)
BP: response to stimulus	2.62E-12
CC: cell wall	1.95E-05
MF: transcription factor activity	4.01E-05

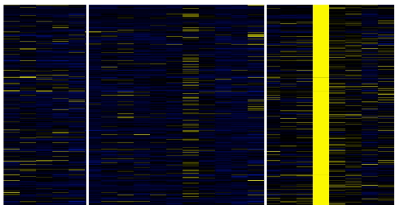

Cluster 6 (phloem CC shoot), 249 genes	P(adj)
MF: arsenate reductase (glutaredoxin) activity	2.92E-12
MF: thiol-disulfide exchange intermediate activity	3.75E-09
MF: transcription factor activity	2.50E-03

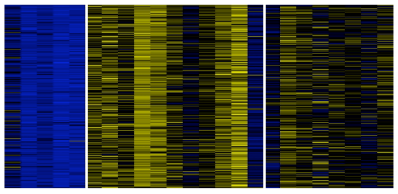

Cluster 12 (translation), 228 genes	P(adj)
MF: structural constituent of ribosome	6.28E-130
CC: ribonucleoprotein complex	4.30E-105
BP: translation	1.50E-75

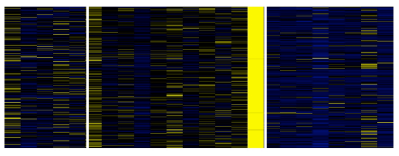

Cluster 15 (older cortex), 207 genes	P(adj)
MF: oxidoreductase activity, acting on paired donors	1.83E-07
BP: phenylpropanoid metabolic process	6.20E-07
MF: transferase activity	2.70E-06

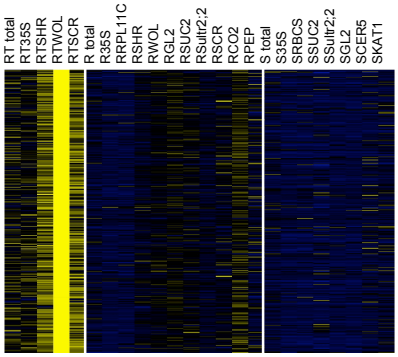

Cluster 18 (RT stele *pWOL*), 353 genes	P(adj)
MF: protein binding	1.10E-06
BP: protein amino acid phosphorylation	1.12E-04
BP: defense response	1.05E-03

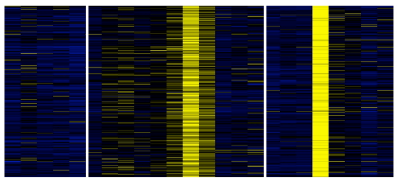

Cluster 22 (phloem CC), 213 genes	P(adj)
BP: ubiquitin-dependent protein catabolic process	3.85E-04
MF: actin binding	1.30E-03
MF: alcohol transmembrane transporter activity	9.49E-03

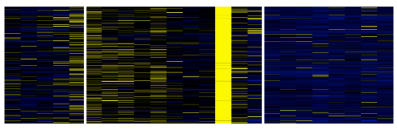

Cluster 25 (mature endodermis), 146 genes	P(adj)
CC: intercellular junction	3.39E-03
CC: anchored to membrane	3.55E-03
BP: fatty acid biosynthetic process	5.30E-03
MF: lipid binding	6.14E-03

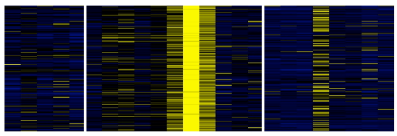

Cluster 30 (root phloem), 157 genes	P(adj)
BP: hormone biosynthetic process	1.18E-04
MF: 1-aminocyclopropane-1-carboxylate oxidase activity	9.68E-04
MF: phospholipase C activity	4.85E-03
BP: response to chemical stimulus	5.61E-03

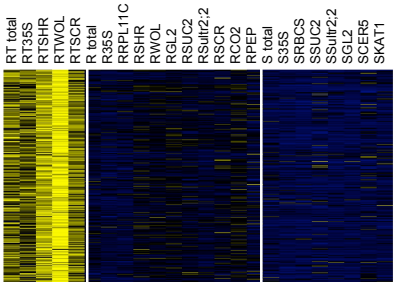

Cluster 41 (stele RT), 265 genes	P(adj)
MF: structural constituent of cell wall	1.12E-07
MF: zinc ion binding	2.29E-04
BP: cellulose and pectin-containing cell wall organization and biogenesis	7.43E-04

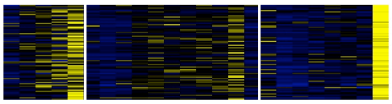

Cluster 50 (guard cells), 74 genes	P(adj)
MF: nucleoside-triphosphatase activity	9.24E-04
BP: RNA interference, production of ta-siRNAs	4.64E-03
BP: proteolysis	7.37E-03

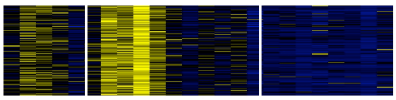

Cluster 53 (stele), 113 genes	P(adj)
BP: lipid transport	4.76E-07
CC: anchored to membrane	1.25E-04
BP: cellulose and pectin-containing secondary cell wall biogenesis	4.24E-04
MF: copper ion binding	2.93E-03

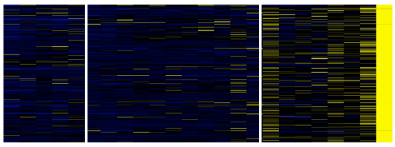

Cluster 54 (guard cells), 172 genes	P(adj)
MF: ATPase activity	1.43E-03
BP: virus induced gene silencing	3.04E-03
MF: 3-methyl-2-oxobutanoate dehydrogenase activity	5.96E-03
BP: stomatal movement	2.15E-02

Fig. S6. GO enrichment in specific cell types (larger version of Fig. 2*B*). mRNAs enriched or depleted in the cell types tested were identified by a differential gene expression analysis between cell types of each organ/region. GO categories enriched or depleted in each mRNA population were identified. Blue: GO categories of enriched genes, $-\log_{10}$ adjusted P-values; red: GO categories of depleted genes, $+\log_{10}$ adjusted P-values. Grey: overlap of GO of enriched and depleted genes. Dataset S2 contains the corresponding expression and GO data. MS: *pSultr2;2* was treated as a plastid containing cell type (bundle sheath); ST: *pSultr2;2* was treated as vasculature cell type.

Fig. S6

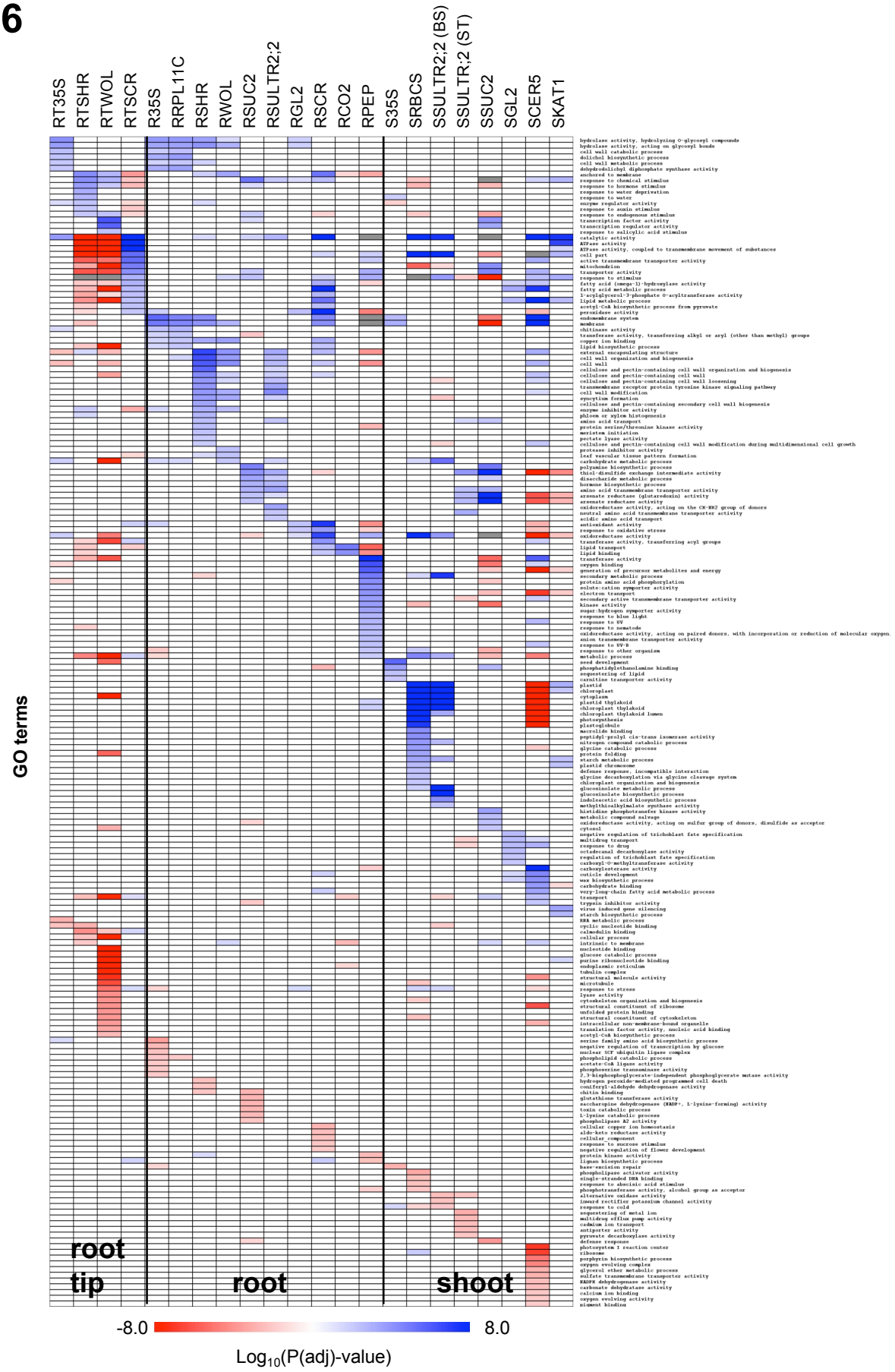
RT35S
RTSHR
RTWOL
RTSCR
R35S
RRPL11C
RSHR
RWOL
RSUC2
RSULTR2;2
RGL2
RSCR
RCO2
RPEP
S35S
SRBCS
SSULTR2;2 (BS)
SSULTR;2 (ST)
SSUC2
SGL2
SCER5
SKAT1
GO terms
root tip
root
shoot
-8.0
8.0
Log10(P(adj)-value)

Fig. S7. Comparison of cell-specific enrichment of polysomal mRNAs with published data on cell-specific gene expression. (*A*) Overlap in cell-type specific mRNA populations obtained by immunopurification of mRNA-ribosome complexes or sorting of GFP-tagged cells. Comparison of enriched mRNAs identified from polysomal mRNA populations with those identified from total mRNA isolated from cells expressing GFP under the control of *pSUC2* (root phloem companion cells), *pPEP* (root elongating and mature cortex), *pSCR* (root epidermis) and *pWOL* (root stele). mRNAs that were significantly enriched in these cell types from Brady et al. (*25*) (reanalyzed in this study, see Dataset S4, sheet *a*; yellow) were compared to those identified in this study (Dataset S2, sheet *a*; grey). Venn diagrams represent the overlap in enriched mRNAs for the three promoters. GO enrichment was determined for each dataset (A: This study, Dataset S2; B: re-analyzed in this study, Dataset S4, sheet *b*). (*B*) Overlap in cell-type specific mRNA populations obtained by polysome immunopurification in shoots or isolation of cell types by other methods. Comparison of enriched mRNAs identified from polysomal mRNA populations with those identified from total mRNA isolated from stem epidermal peels (*21*), protoplasted guard cells (*22*), isolated trichomes (*23*), or isolated phloem companion cells of seedling root hypocotyls (*24*). mRNAs that were significantly enriched in these cell types (reanalyzed in this study from .CEL files, see Dataset S4, sheet *d*; yellow) were compared to those identified in this study (Dataset S2, sheet *a*; grey). Venn diagrams represent the overlap in enriched mRNAs for the two cell types. GO enrichment determined for each dataset (A: This study, Dataset S2; B: re-analyzed in this study, Dataset S4, sheet *e*).

Root populations

Fig. S7A

pSUC2

Brady et al. 2007

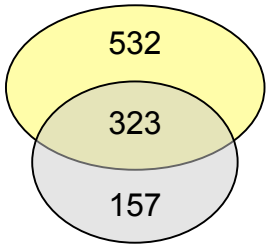

GOID	Term	Ont	P(adj) (A)	(Padj) (B)
GO:0042221	response to chemical stimulus	BP	8.06E-06	3.97E-04
GO:0006596	polyamine biosynthetic process	BP	2.06E-05	1.82E-02
GO:0030508	thiol-disulfide exchange intermediate activity	MF	8.23E-05	9.13E-05
GO:0005984	disaccharide metabolic process	BP	3.30E-04	2.55E-02
GO:0042446	hormone biosynthetic process	BP	9.76E-04	1.48E-03
GO:0015171	amino acid transmembrane transporter activity	MF	1.22E-03	2.78E-02
GO:0008794	arsenate reductase (glutaredoxin) activity	MF	4.88E-03	4.19E-03
GO:0030611	arsenate reductase activity	MF	6.56E-03	3.18E-04
GO:0005215	transporter activity	MF	1.07E-02	1.61E-02
GO:0003700	transcription factor activity	MF	4.01E-02	4.74E-14
GO:0005634	nucleus	CC	6.44E-02	4.97E-04

pPEP

Brady et al. 2007

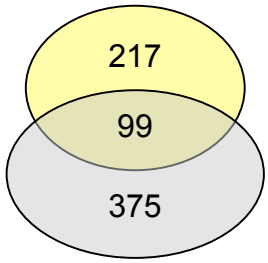

GOID	Term	Ont	P(adj)(A)	(Padj) (B)
GO:0003824	catalytic activity	MF	2.51E-13	1.90E-13
GO:0016020	membrane	CC	5.10E-12	1.75E-11
GO:0019825	oxygen binding	MF	4.33E-07	4.05E-05
GO:0006091	generation of precursor metabolites and energy	BP	1.44E-06	8.70E-04
GO:0019748	secondary metabolic process	BP	1.22E-05	2.98E-03
GO:0015294	solute:cation symporter activity	MF	9.35E-05	9.73E-07
GO:0006118	electron transport	BP	1.03E-04	1.99E-02
GO:0005351	sugar:hydrogen symporter activity	MF	3.57E-04	4.78E-08
GO:0005215	transporter activity	MF	7.71E-04	9.87E-04
GO:0009637	response to blue light	BP	1.48E-03	1.64E-04
GO:0009624	response to nematode	BP	2.11E-03	1.20E-04
GO:0010224	response to UV-B	BP	4.73E-03	1.10E-02
GO:0009416	response to light stimulus	BP	1.13E-02	3.98E-07

pSCR

Brady et al. 2007

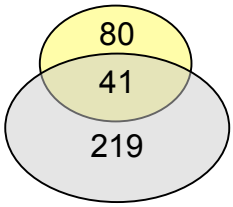

GOID	Term	Ont	P(adj)(A)	(Padj) (B)
GO:0003824	catalytic activity	MF	2.12E-09	7.49E-04
GO:0004601	peroxidase activity	MF	9.76E-09	6.68E-06
GO:0012505	endomembrane system	CC	4.01E-05	1.22E-02
GO:0006979	response to oxidative stress	BP	1.68E-04	5.48E-04
GO:0042221	response to chemical stimulus	BP	3.29E-03	4.82E-04

pWOL

Brady et al. 2007

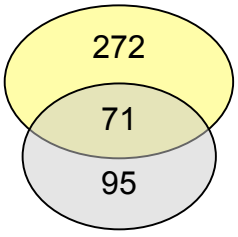

GOID	Term	Ont	P(adj) (A)	P(adj) (B)
GO:0005618	cell wall	CC	6.71E-05	7.58E-05
GO:0030312	external encapsulating structure	CC	7.77E-05	1.79E-05
GO:0005507	copper ion binding	MF	2.30E-04	1.73E-06
GO:0031225	anchored to membrane	CC	4.32E-04	2.20E-06
GO:0016798	hydrolase activity, acting on glycosyl bonds	MF	1.30E-03	1.05E-03
GO:0016020	membrane	CC	1.95E-03	6.19E-05
GO:0010305	leaf vascular tissue pattern formation	BP	5.53E-03	5.64E-02
GO:0009505	cellulose and pectin-containing cell wall	CC	1.92E-02	1.16E-02
GO:0044262	cellular carbohydrate metabolic process	BP	7.93E-02	9.20E-04
GO:0006869	lipid transport	BP	9.42E-02	4.46E-04

Shoot populatons

Fig. S7B

pCER5

Suh et al. 2005

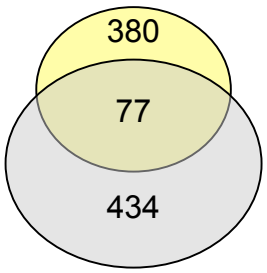

GOID	Term	Ont	P(adj) (A)	P(adj) (B)
GO:0016020	membrane	CC	2.86E-22	5.50E-10
GO:0012505	endomembrane system	CC	2.16E-14	1.18E-02
GO:0016740	transferase activity	MF	1.07E-06	9.58E-09
GO:0042335	cuticle development	BP	2.91E-05	1.26E-02
GO:0010025	wax biosynthetic process	BP	6.53E-05	1.90E-03
GO:0030246	carbohydrate binding	MF	1.50E-04	6.49E-05
GO:0005618	cell wall	CC	1.97E-03	1.37E-06
GO:0050896	response to stimulus	BP	3.50E-03	2.09E-17
GO:0009505	cellulose and pectin-containing cell wall	CC	5.22E-03	1.27E-04
GO:0042221	response to chemical stimulus	BP	2.39E-02	2.61E-07

pKAT1

Yang et al. 2008

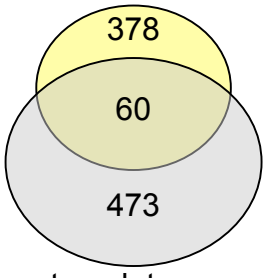

GOID	Term	Ont	P(adj) (A)	P(adj) (B)
GO:0016887	ATPase activity	MF	1.53E-07	9.00E-02
GO:0006629	lipid metabolic process	BP	2.70E-03	4.46E-02

pGL2

Jacoby et al. 2008

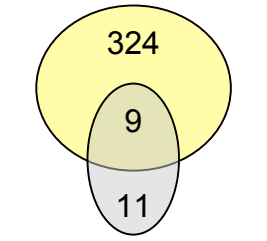

GOID	Term	Ont	P(adj) (A)	P(adj) (B)
GO:0010062	negative regulation of trichoblast fate specification	BP	2.12E-03	7.16E-01
GO:0010061	regulation of trichoblast fate specification	BP	6.36E-03	2.62E-02

pSUC2

Zhao et al. 2005

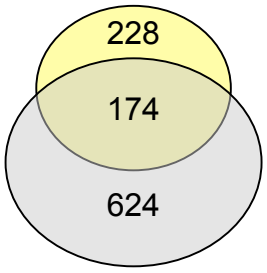

GOID	Term	Ont	P(adj) (A)	P(adj) (B)
GO:0030611	arsenate reductase activity	MF	1.56E-12	3.14E-03
GO:0030508	thiol-disulfide exchange intermediate activity	MF	1.08E-11	1.47E-04
GO:0008794	arsenate reductase (glutaredoxin) activity	MF	3.98E-11	2.33E-03
GO:0003700	transcription factor activity	MF	1.06E-04	1.52E-02
GO:0042221	response to chemical stimulus	BP	4.26E-03	1.04E-05
GO:0006865	amino acid transport	BP	5.93E-03	2.81E-03
GO:0016765	transferase activity, transferring alkyl or aryl (other than methyl) groups	MF	7.75E-02	2.13E-02
GO:0050896	response to stimulus	BP	9.64E-02	8.32E-06

Fig. S7C

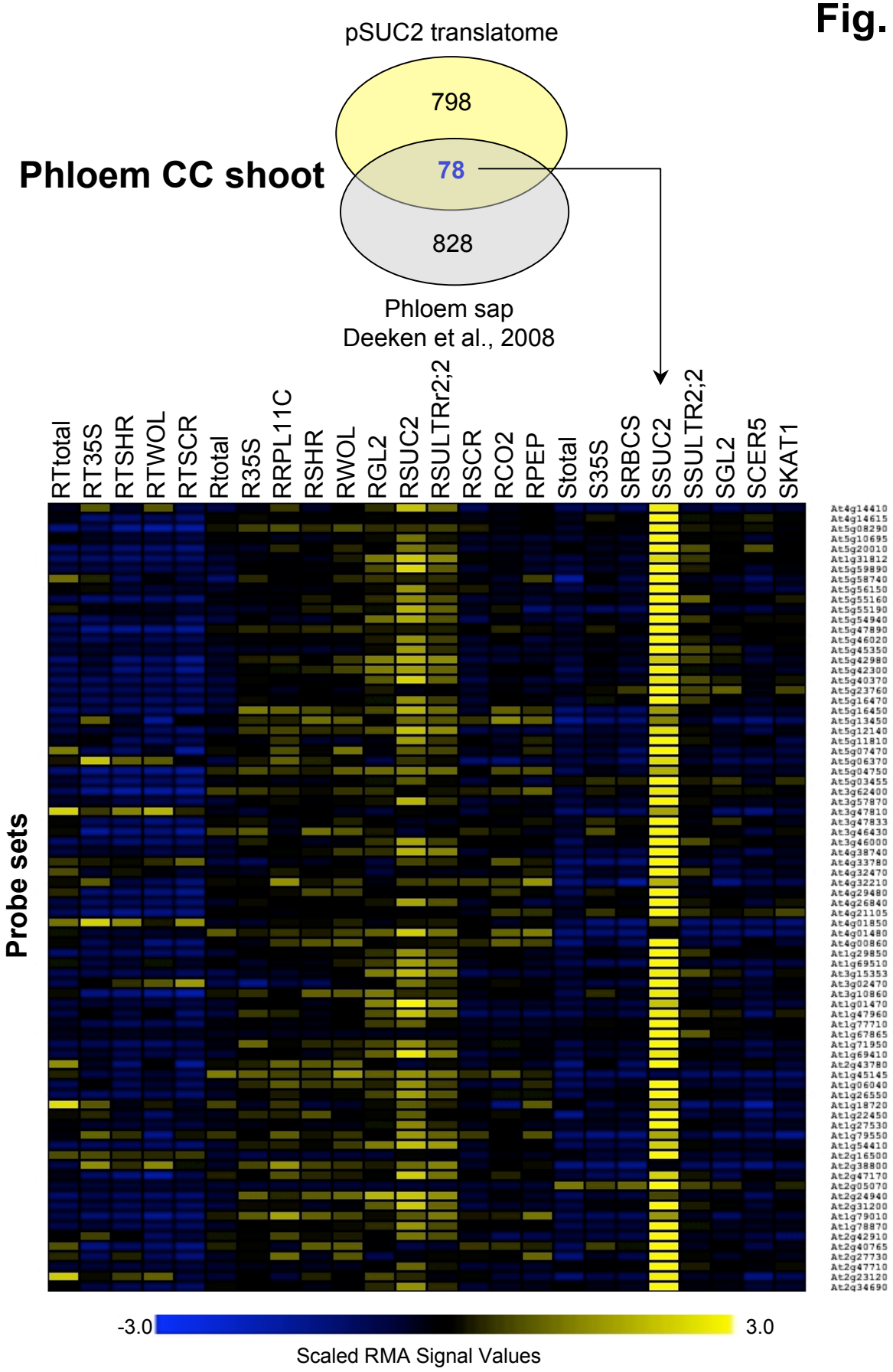
pSUC2 translatome
798
78
828
Phloem CC shoot
Phloem sap
Deeken et al., 2008
RTtotal
RT35S
RTSHR
RTWOL
RTSCR
Rtotal
R35S
RRPL11C
RSHR
RWOL
RGL2
RSUC2
RSULTRr2;2
RSCR
RCO2
RPEP
Stotal
S35S
SRBCS
SSUC2
SSULTR2;2
SGL2
SCER5
SKAT1
Probe sets
-3.0
3.0
Scaled RMA Signal Values

Fig. S8. mRNAs immunopurified with promoters that target the same cell types are partially overlapping. Overlap of significantly enriched gene lists in partially overlapping cell types (phloem companion cells, *pSUC2* and *pSultr2;2*; root cortex, *pCO2* and *pPEP*). Data are from Dataset S2, sheet *a*. The GO annotation enrichment was obtained for the overlapping phloem-companion cell specific gene lists of roots and shoots, and for the distinct cortex-specific gene lists.

Fig. S8

Phloem CC root

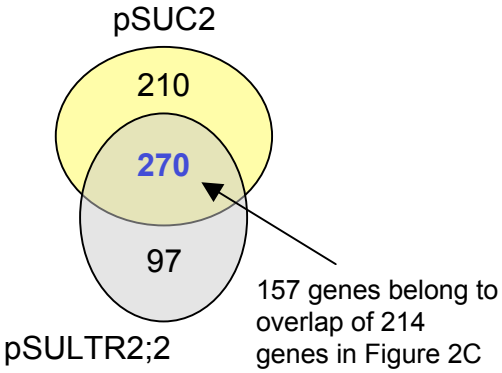

GOID	Term	Ont	P(adj)
GO:0030508	thiol-disulfide exchange intermediate activity	MF	5.92E-05
GO:0042446	hormone biosynthetic process	BP	2.05E-04
GO:0015171	amino acid transmembrane transporter activity	MF	1.82E-03
GO:0035251	UDP-glucosyltransferase activity	MF	6.12E-03
GO:0009815	1-aminocyclopropane-1-carboxylate oxidase activity	MF	8.94E-03
GO:0030422	RNA interference, production of siRNA	BP	1.04E-02
GO:0008794	arsenate reductase (glutaredoxin) activity	MF	1.46E-02
GO:0005985	sucrose metabolic process	BP	1.89E-02
GO:0010305	leaf vascular tissue pattern formation	BP	1.98E-02
GO:0015804	neutral amino acid transport	BP	3.28E-02
GO:0004629	phospholipase C activity	MF	4.37E-02

Phloem CC shoot

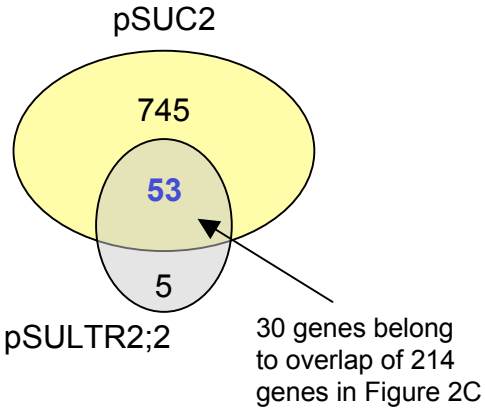

GOID	Term	Ont	P(adj)
GO:0030508	thiol-disulfide exchange intermediate activity	MF	6.94E-05
GO:0015175	neutral amino acid transmembrane transporter activity	MF	4.53E-04
GO:0008794	arsenate reductase (glutaredoxin) activity	MF	1.46E-03
GO:0009915	phloem loading	BP	2.24E-02
GO:0006537	glutamate biosynthetic process	BP	2.99E-02
GO:0030418	nicotianamine biosynthetic process	BP	2.99E-02
GO:0006021	inositol biosynthetic process	BP	3.73E-02
GO:0015804	neutral amino acid transport	BP	3.73E-02

Cortex root

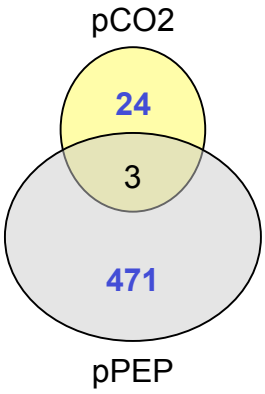

GOID	Term	Ont	P(adj)
pCO2			
GO:0006869	lipid transport	BP	1.06E-05
GO:0008289	lipid binding	MF	7.72E-05
pPEP			
GO:0003824	catalytic activity	MF	2.51E-13
GO:0016020	membrane	CC	5.10E-12
GO:0019825	oxygen binding	MF	4.33E-07
GO:0006091	generation of precursor metabolites and energy	BP	1.44E-06
GO:0019748	secondary metabolic process	BP	1.22E-05
GO:0006468	protein amino acid phosphorylation	BP	6.02E-05
GO:0015294	solute:cation symporter activity	MF	9.35E-05
GO:0009637	response to blue light	BP	1.48E-03
GO:0009624	response to nematode	BP	2.11E-03
GO:0010224	response to UV-B	BP	4.73E-03

Fig. S9. GO enrichment in cell type mRNA populations after hypoxic treatment. After selection of hypoxia-modified genes by pairwise comparison of hypoxia versus control for each cell type (Dataset S5), the GO enrichment P-value of all GO terms was calculated by the GOHyperGAll function (*27*). Overlapping GO terms were removed by the simplify variant of the function. Data shown are $\log_{10}$ of adjusted P-values. (*A*) Blue, GO enrichment of hypoxia-induced genes; (*B*) Red, GO enrichment of hypoxia-reduced genes.

Fig. S9A

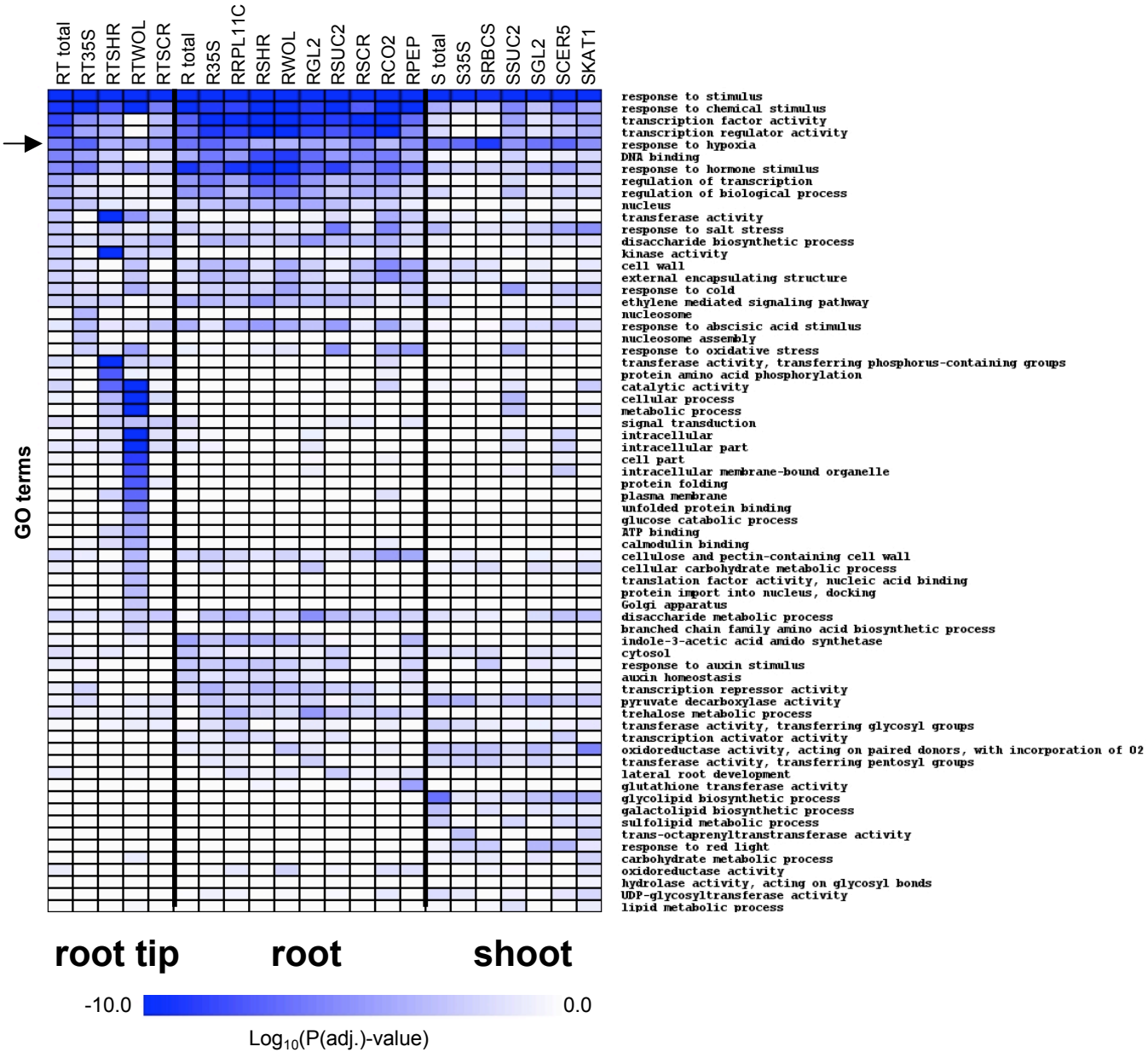
RT total
RT35S
RTSHR
RTWOL
RTSCR
R total
R35S
RRPL11C
RSHR
RWOL
RGL2
RSUC2
RSCR
RCO2
RPEP
S total
S35S
SRBCS
SSUC2
SGL2
SCER5
SKAT1
GO terms
response to stimulus
response to chemical stimulus
transcription factor activity
transcription regulator activity
response to hypoxia
DNA binding
response to hormone stimulus
regulation of transcription
regulation of biological process
nucleus
transferase activity
response to salt stress
disaccharide biosynthetic process
kinase activity
cell wall
external encapsulating structure
response to cold
ethylene mediated signaling pathway
nucleosome
response to abscisic acid stimulus
nucleosome assembly
response to oxidative stress
transferase activity, transferring phosphorus-containing groups
protein amino acid phosphorylation
catalytic activity
cellular process
metabolic process
signal transduction
intracellular
intracellular part
cell part
intracellular membrane-bound organelle
protein folding
plasma membrane
unfolded protein binding
glucose catabolic process
ATP binding
calmodulin binding
cellulose and pectin-containing cell wall
cellular carbohydrate metabolic process
translation factor activity, nucleic acid binding
protein import into nucleus, docking
Golgi apparatus
disaccharide metabolic process
branched chain family amino acid biosynthetic process
indole-3-acetic acid amido synthetase
cytosol
response to auxin stimulus
auxin homeostasis
transcription repressor activity
pyruvate decarboxylase activity
trehalose metabolic process
transferase activity, transferring glycosyl groups
transcription activator activity
oxidoreductase activity, acting on paired donors, with incorporation of O2
transferase activity, transferring pentosyl groups
lateral root development
glutathione transferase activity
glycolipid biosynthetic process
galactolipid biosynthetic process
sulfolipid metabolic process
trans-octaprenyltranstransferase activity
response to red light
carbohydrate metabolic process
oxidoreductase activity
hydrolase activity, acting on glycosyl bonds
UDP-glycosyltransferase activity
lipid metabolic process
root tip
root
shoot
-10.0
0.0
Log10(P(adj.)-value)

Fig. S9B


RT total
RT35S
RTSHR
RTWOL
RTSCR
R total
R35S
RRPL11C
RSHR
RWOL
RGL2
RSUC2
RSCR
RCO2
RPEP
S total
S35S
SRBCS
SSUC2
SGL2
SCER5
SKAT1
GO terms
membrane
endomembrane system
transmembrane receptor protein tyrosine kinase signaling pathway
catalytic activity
external encapsulating structure
cell wall
cell part
transferase activity
peroxidase activity
cell wall organization and biogenesis
antioxidant activity
response to oxidative stress
cell wall modification
trichoblast differentiation
root development
growth
apoplast
indole glucosinolate biosynthetic process
structural constituent of cell wall
carboxylesterase activity
anchored to membrane
response to red light
cellulose and pectin-containing cell wall
signal transduction
cellulose and pectin-containing cell wall modification
cellulose and pectin-containing cell wall loosening
nitrogen compound biosynthetic process
cellulose and pectin-containing cell wall modification during multidimensional cell growth
transferase activity, transferring glycosyl groups
cell wall modification during multidimensional cell growth
response to chemical stimulus
response to stimulus
glucan metabolic process
cellular polysaccharide metabolic process
pectinesterase inhibitor activity
transcription factor activity
transcription regulator activity
response to abscisic acid stimulus
response to hormone stimulus
DNA binding
cytoskeletal protein binding
autophagy
copper ion binding
oxygen binding
dicarboxylic acid metabolic process
lipid metabolic process
aromatic amino acid family metabolic process
oligopeptide transport
protein serine/threonine kinase activity
kinase activity
protein amino acid phosphorylation
unidimensional cell growth
transferase activity, transferring phosphorus-containing groups
hydrolase activity, acting on glycosyl bonds
multidimensional cell growth
carbohydrate metabolic process
cellular carbohydrate metabolic process
regulation of cell size
glucosinolate biosynthetic process
cellular process
metabolic process
intracellular part
intracellular
Golgi apparatus
amino acid biosynthetic process
S-adenosylmethionine biosynthetic process
ATP binding
longitudinal axis specification
phloem or xylem histogenesis
cytokinin mediated signaling
response to cytokinin stimulus
histidine phosphotransfer kinase activity
protein phosphatase type 2A complex
protein phosphatase type 2A regulator activity
cellulose and pectin-containing primary cell wall biogenesis
nucleus
carnitine transporter activity
regulation of biological process
regulation of transcription
aging
leaf development
adenylyl-sulfate reductase activity
sulfate assimilation
sulfate reduction, APS pathway
response to auxin stimulus
UDP-glycosyltransferase activity
auxin:hydrogen symporter activity
virus induced gene silencing
DNA polymerase III complex
plasma membrane
meristem maintenance
regulation of meristem growth
guanyl-nucleotide exchange factor activity
ribosome
structural constituent of ribosome
ribosome biogenesis and assembly
root tip
root
shoot
-10.0
0.0
Log10(P(adj.)-value)

Fig. S10. Pattern of cell-type specific gene expression under hypoxia across all organs. (*A*) Means of RMA-normalized data of 6,461 genes (probe pair sets) of control and hypoxia samples were sorted by fuzzy k-means clustering, and the median of each cluster was calculated from scaled expression values. White bars divide different organs. The 100 clusters obtained from clustering of the data were then sorted to visualize trends in individual cell-types. Red arrows: clusters with reduced genes, presented in *B*; blue arrows: clusters with induced genes, presented in *C*. (*B* and *C*) Examples of different response clusters are shown, with scaled RMA-values for all genes in the clusters, and a table of the three most significant GO terms. Dataset S6 contains the cluster and GO data.

Fig. S10A

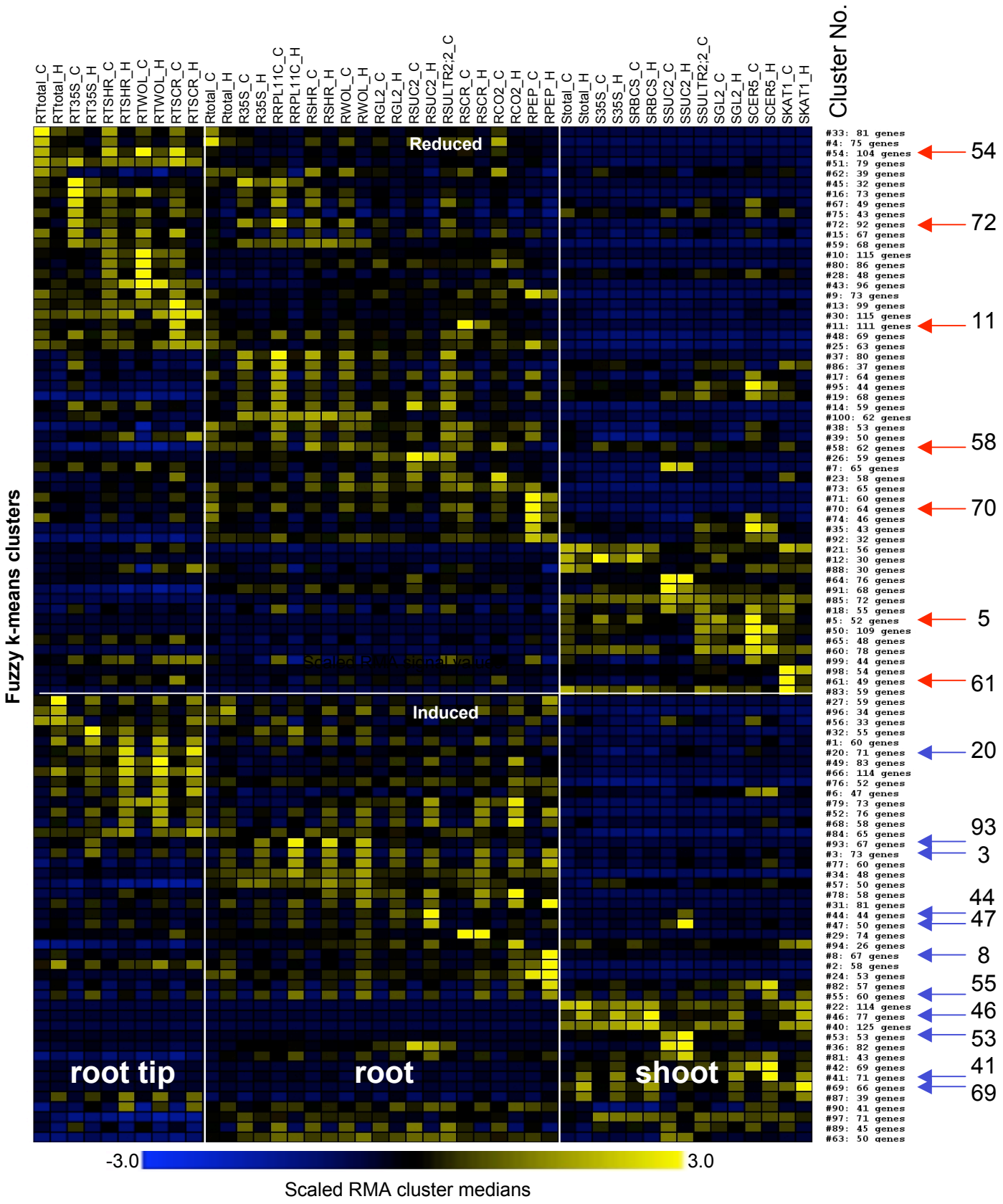
RTtotal_C
RTtotal_H
RT35S_C
RT35S_H
RTSHR_C
RTSHR_H
RTWOL_C
RTWOL_H
RTSCR_C
RTSCR_H
Rtotal_C
Rtotal_H
R35S_C
R35S_H
RRPL11C_C
RRPL11C_H
RSHR_C
RSHR_H
RWOL_C
RWOL_H
RGL2_C
RGL2_H
RSUC2_C
RSUC2_H
RSULTR2;2_C
RSCR_C
RSCR_H
RCO2_C
RCO2_H
RPEP_C
RPEP_H
Stotal_C
Stotal_H
S35S_C
S35S_H
SRBCS_C
SRBCS_H
SSUC2_C
SSUC2_H
SSULTR2;2_C
SGL2_C
SGL2_H
SCER5_C
SCER5_H
SKAT1_C
SKAT1_H
Cluster No.
Reduced
Induced
Fuzzy k-means clusters
root tip
root
shoot
-3.0
3.0
Scaled RMA cluster medians
#33: 81 genes
#4: 75 genes
#54: 104 genes
#51: 79 genes
#62: 39 genes
#45: 32 genes
#16: 73 genes
#67: 49 genes
#75: 43 genes
#72: 92 genes
#15: 67 genes
#59: 68 genes
#10: 115 genes
#80: 86 genes
#28: 48 genes
#43: 96 genes
#9: 73 genes
#13: 99 genes
#30: 115 genes
#11: 111 genes
#48: 69 genes
#25: 63 genes
#37: 80 genes
#86: 37 genes
#17: 64 genes
#95: 44 genes
#19: 68 genes
#14: 59 genes
#100: 62 genes
#38: 53 genes
#39: 50 genes
#58: 62 genes
#26: 59 genes
#7: 65 genes
#23: 58 genes
#73: 65 genes
#71: 60 genes
#70: 64 genes
#74: 46 genes
#35: 43 genes
#92: 32 genes
#21: 56 genes
#12: 30 genes
#88: 30 genes
#64: 76 genes
#91: 68 genes
#85: 72 genes
#18: 55 genes
#5: 52 genes
#50: 109 genes
#65: 48 genes
#60: 78 genes
#99: 44 genes
#98: 54 genes
#61: 49 genes
#83: 59 genes
#27: 59 genes
#96: 34 genes
#56: 33 genes
#32: 55 genes
#1: 60 genes
#20: 71 genes
#49: 83 genes
#66: 114 genes
#76: 52 genes
#6: 47 genes
#79: 73 genes
#52: 76 genes
#68: 58 genes
#84: 65 genes
#93: 67 genes
#3: 73 genes
#77: 60 genes
#34: 48 genes
#57: 50 genes
#78: 58 genes
#31: 81 genes
#44: 44 genes
#47: 50 genes
#29: 74 genes
#94: 26 genes
#8: 67 genes
#2: 58 genes
#24: 53 genes
#82: 57 genes
#55: 60 genes
#22: 114 genes
#46: 77 genes
#40: 125 genes
#53: 53 genes
#36: 82 genes
#81: 43 genes
#42: 69 genes
#41: 71 genes
#69: 66 genes
#87: 39 genes
#90: 41 genes
#97: 71 genes
#89: 45 genes
#63: 50 genes
54
72
11
58
70
5
61
20
93
3
44
47
8
55
46
53
41
69

Fig. S10B - reduced genes

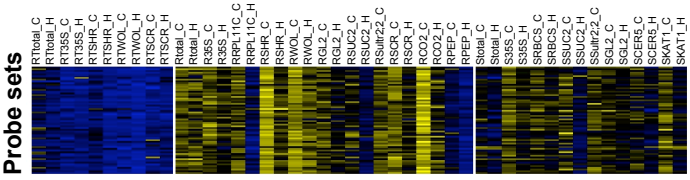

Cluster 58, 62 genes (ribosomal proteins)	P(adj)
MF: structural constituent of ribosome	1.04E-51
CC: ribosome	4.98E-47
BP: translation	9.48E-29

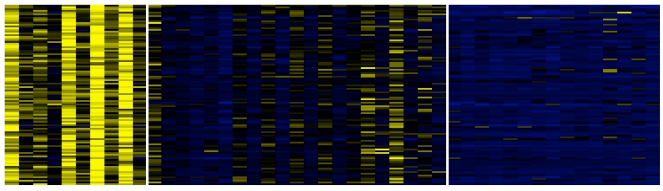

Cluster 54, 104 genes (reduction in root tip)	P(adj)
MF: structural constituent of cell wall	1.49E-07
BP: cellulose and pectin-containing cell wall organization and biogenesis	8.63E-04
BP: trichoblast differentiation	1.58E-03

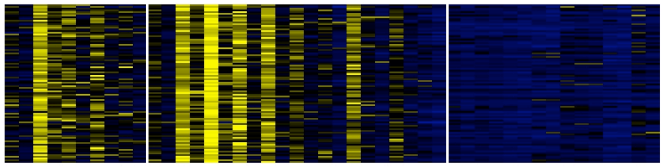

Cluster 72, 92 genes (reduction of stele-enriched genes)	P(adj)
BP: glucosinolate biosynthetic process	3.61E-06
BP: tryptophan catabolic process	1.68E-04
BP: auxin biosynthetic process	4.82E-04

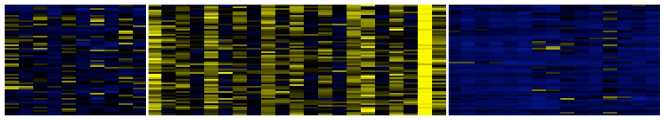

Cluster 70, 64 genes (reduction of cortex-enriched genes)	P(adj)
MF: transferase activity, transferring glycosyl groups	6.33E-03
BP: chalcone biosynthetic process	2.65E-02
BP: response to boron	2.65E-02

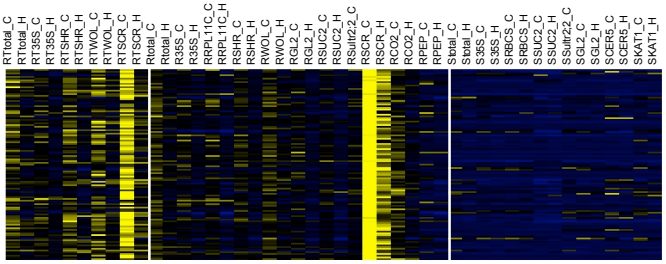

Cluster 11, 111 genes (reduction of endodermis-enriched genes)	P(adj)
MF: catalytic activity	8.98E-08
BP: monocarboxylic acid metabolic process	1.75E-06
MF: copper ion binding	2.73E-03

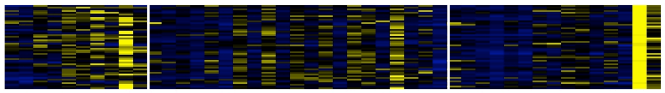

Cluster 61, 49 genes (reduction of guard cell-enriched genes)	P(adj)
CC: DNA polymerase III complex	2.41E-04
CC: protein phosphatase type 2A complex	2.51E-03
MF: protein phosphatase type 2A regulator activity	2.68E-03

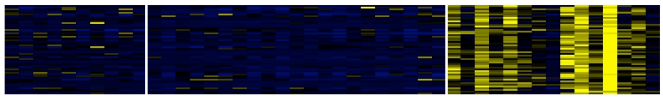

Cluster 5, 52 genes (reduction of epidermis-enriched genes)	P(adj)
BP: response to auxin stimulus	3.31E-07
MF: glucuronosyltransferase activity	1.24E-03
CC: lateral plasma membrane	6.85E-03

Fig. S10C - induced genes

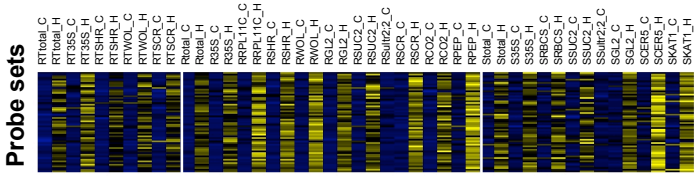

Cluster 55, 60 genes (hypoxic induction in all cell types)	P(adj)
BP: response to far red light	1.35E-04
MF: 4-hydroxyphenylpyruvate dioxygenase activity	1.47E-02
MF: calcium-dependent protein serine/threonine kinase activity	1.47E-02

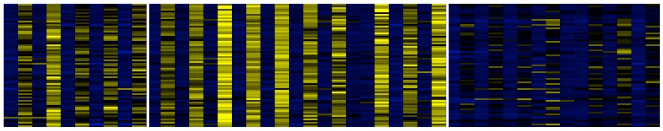

Cluster 3, 73 genes (hypoxic induction in all root CTs)	P(adj)
BP: response to hypoxia	3.45E-05
MF: pyruvate decarboxylase activity	1.56E-03
MF: sucrose synthase activity	1.56E-03

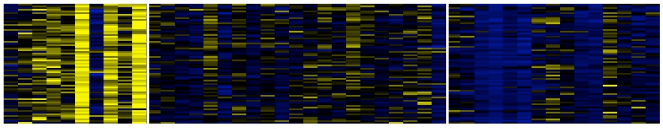

Cluster 20, 71 genes (induction in root tip)	P(adj)
BP: cellular process	5.36E-05
MF: DNA-dependent ATPase activity	1.96E-02
MF: methionine-tRNA ligase activity	3.41E-02

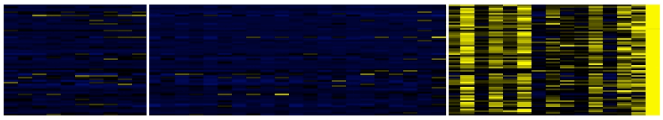

Cluster 69, 66 genes (induction in guard cells)	P(adj)
BP: glycolipid biosynthetic process	9.61E-06
BP: cellular response to phosphate starvation	6.18E-05
BP: sulfolipid metabolic process	7.43E-05

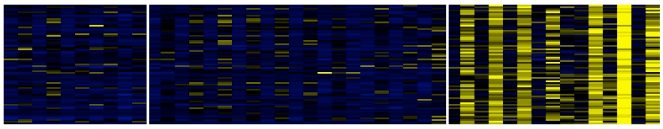

Cluster 41, 71 genes (hypoxic induction in shoot CTs)	P(adj)
BP: response to stimulus	1.25E-08
BP: galactolipid biosynthetic process	2.93E-03
MF: transcription factor activity	1.14E-02

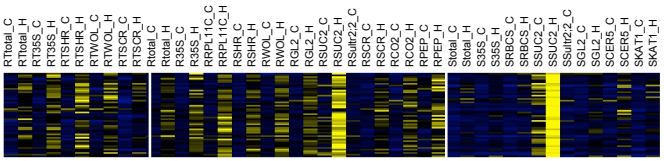

Cluster 47, 50 genes (induction in phloem CC)	P(adj)
BP: response to heat	4.91E-12
MF: transcription activator activity	5.55E-03
BP: response to water deprivation	1.34E-02

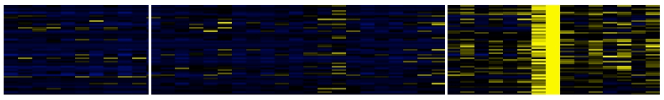

Cluster 53, 53 genes (induction in shoot phloem CC)	P(adj)
BP: regulation of timing of meristematic phase transition	1.29E-05
MF: oligopeptide transporter activity	3.80E-03
MF: transcription factor activity	8.84E-03

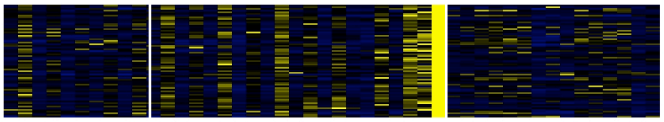

Cluster 8, 67 genes (induction in root cortex)	P(adj)
BP: toxin catabolic process	3.87E-05
MF: glutathione transferase activity	7.38E-05
BP: defense response to fungus	1.28E-04

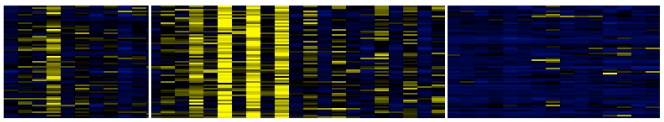

Cluster 93, 67 genes (induction in stele cells)	P(adj)
MF: transcription factor activity	3.89E-04
BP: regulation of transcription	1.00E-03
BP: response to auxin stimulus	1.66E-03

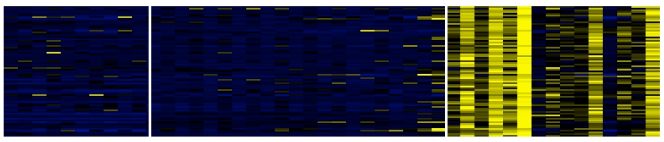

Cluster 46, 77 genes (induction in chloroplast-containing cells)	P(adj)
MF: trans-octaprenyltranstransferase activity	8.05E-05
BP: response to wounding	2.51E-04
MF: dimethylallyltranstransferase activity	8.01E-04

Fig. S11. Heat shock protein (HSP) and heat shock factor (HSF) mRNA adjustments in polysomal mRNA cell type populations after hypoxic treatment. The SLR of pairwise comparisons of hypoxia versus control for each cell type is shown for all genes associated with the heat shock response (names according to ref. *41*). Data are signal-log-ratios between H and C from Dataset S5. Arrows indicate the phloem CC samples (*pSUC2*) that show the highest and most complex induction of HSP mRNAs in the polysomal population.

Fig. S11

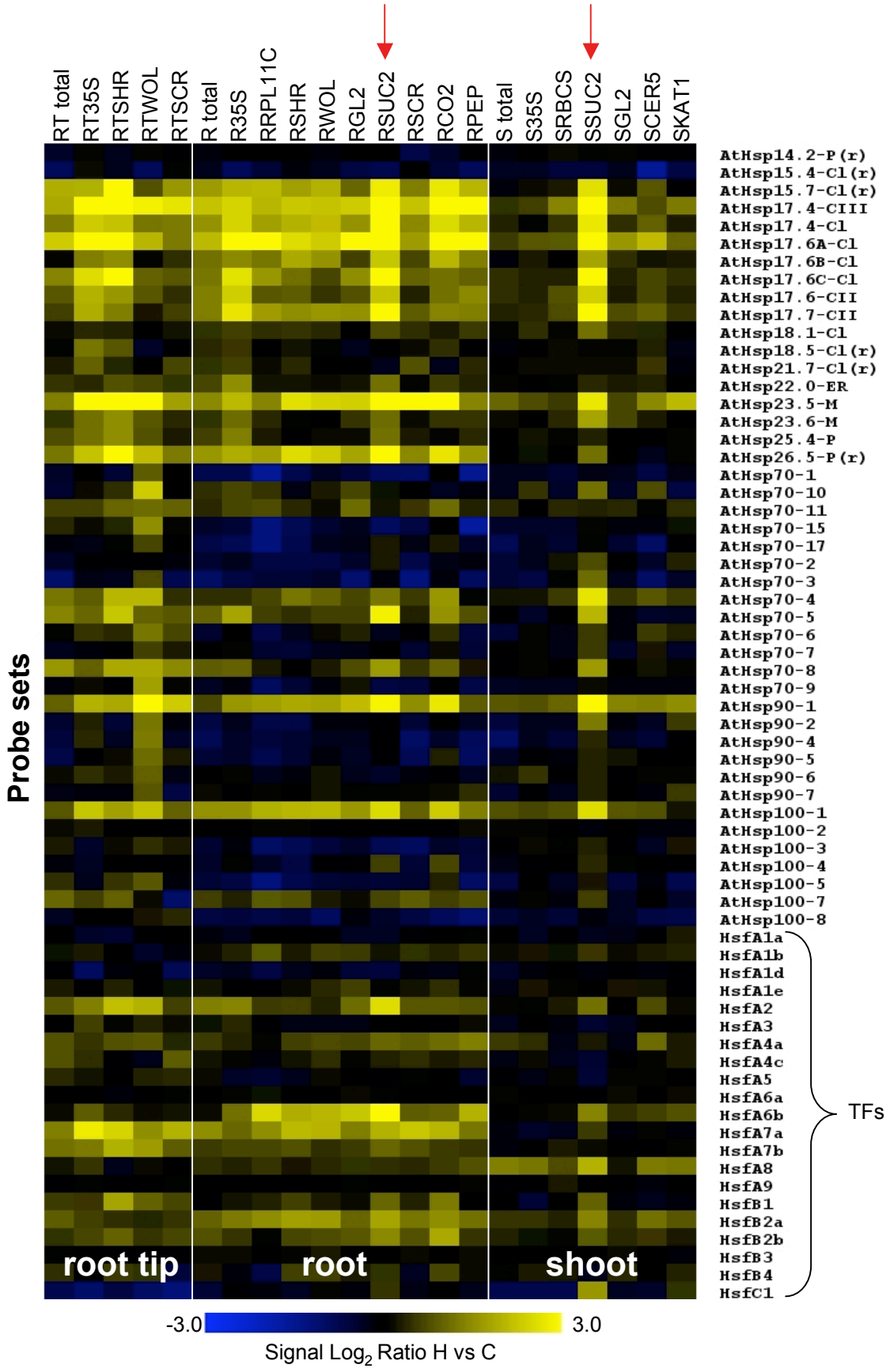
RT total
RT35S
RTSHR
RTWOL
RTSCR
R total
R35S
RRPL11C
RSHR
RWOL
RGL2
RSUC2
RSCR
RCO2
RPEP
S total
S35S
SRBCS
SSUC2
SGL2
SCER5
SKAT1
Probe sets
AtHsp14.2-P(r)
AtHsp15.4-Cl(r)
AtHsp15.7-Cl(r)
AtHsp17.4-CIII
AtHsp17.4-Cl
AtHsp17.6A-Cl
AtHsp17.6B-Cl
AtHsp17.6C-Cl
AtHsp17.6-CII
AtHsp17.7-CII
AtHsp18.1-Cl
AtHsp18.5-Cl(r)
AtHsp21.7-Cl(r)
AtHsp22.0-ER
AtHsp23.5-M
AtHsp23.6-M
AtHsp25.4-P
AtHsp26.5-P(r)
AtHsp70-1
AtHsp70-10
AtHsp70-11
AtHsp70-15
AtHsp70-17
AtHsp70-2
AtHsp70-3
AtHsp70-4
AtHsp70-5
AtHsp70-6
AtHsp70-7
AtHsp70-8
AtHsp70-9
AtHsp90-1
AtHsp90-2
AtHsp90-4
AtHsp90-5
AtHsp90-6
AtHsp90-7
AtHsp100-1
AtHsp100-2
AtHsp100-3
AtHsp100-4
AtHsp100-5
AtHsp100-7
AtHsp100-8
HsfA1a
HsfA1b
HsfA1d
HsfA1e
HsfA2
HsfA3
HsfA4a
HsfA4c
HsfA5
HsfA6a
HsfA6b
HsfA7a
HsfA7b
HsfA8
HsfA9
HsfB1
HsfB2a
HsfB2b
HsfB3
HsfB4
HsfC1
TFs
root tip
root
shoot
-3.0
3.0
Signal Log2 Ratio H vs C

Fig. S12. Cell-type specific gene expression data are valuable to characterize gene families. (*A*) Transcription factor (TF) family member genes are differentially expressed in cell types. All TF families are shown with SLRs generated in the differential gene expression analysis of control samples for all cell types and organs (Dataset S2, sheet *a*). Values were ordered by hierarchical clustering in MEV. MS: *pSultr2;2* was treated as a plastid containing cell type (bundle sheath); ST: *pSultr2;2* was treated as vasculature cell type. (*B*) Focus on three TF families, extracted from *A*. (*C* and *D*) TF family enrichment in specific cell types confirmed by GO analysis. Differentially expressed genes (Dataset S2, sheet *a*) were evaluated for TF families. (*C*) TF family enrichment (TF family gene lists were obtained from TAIR and AGRIS) among the cell-type enriched genes, analyzed for significant enrichment by the GOHyperGAll function (*27*). Data shown are $\log_{10}$ of adjusted P-values. (*D*) Enrichment of binding sites for transcription factors in the -1000 bp promoter region of cell-type enriched genes (analyzed by Athena, http://www.bioinformatics2.wsu.edu/cgi-bin/Athena/cgi/analysis_select.pl). Data are $\log_{10}$ of adjusted P-values.

Fig. S12A

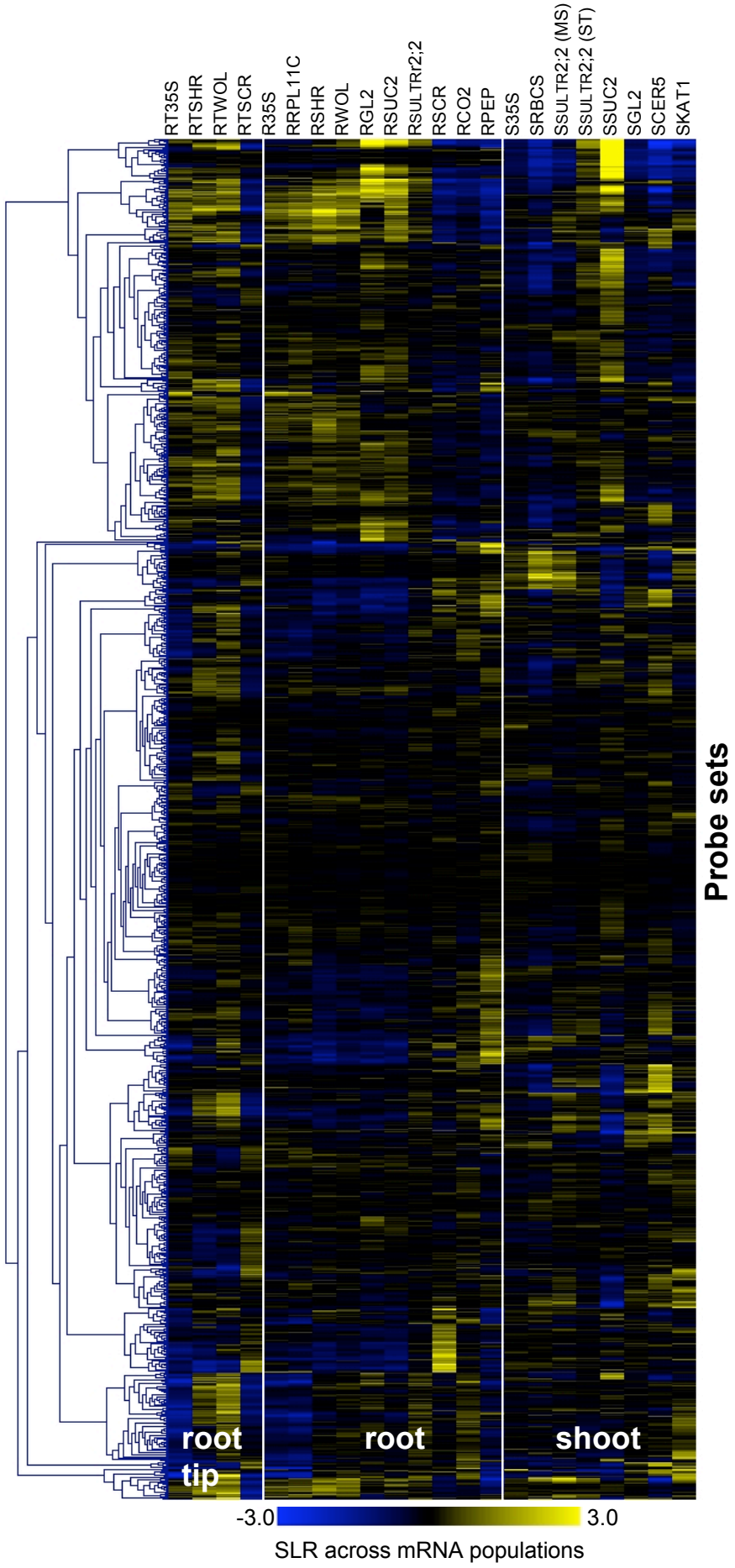
RT35S
RTSHR
RTWOL
RTSCR
R35S
RRPL11C
RSHR
RWOL
RGL2
RSUC2
RSULTRr2;2
RSCR
RCO2
RPEP
S35S
SRBCS
SSULTR2;2 (MS)
SSULTR2;2 (ST)
SSUC2
SGL2
SCER5
SKAT1
root tip
root
shoot
Probe sets
-3.0
3.0
SLR across mRNA populations

Fig. S12B

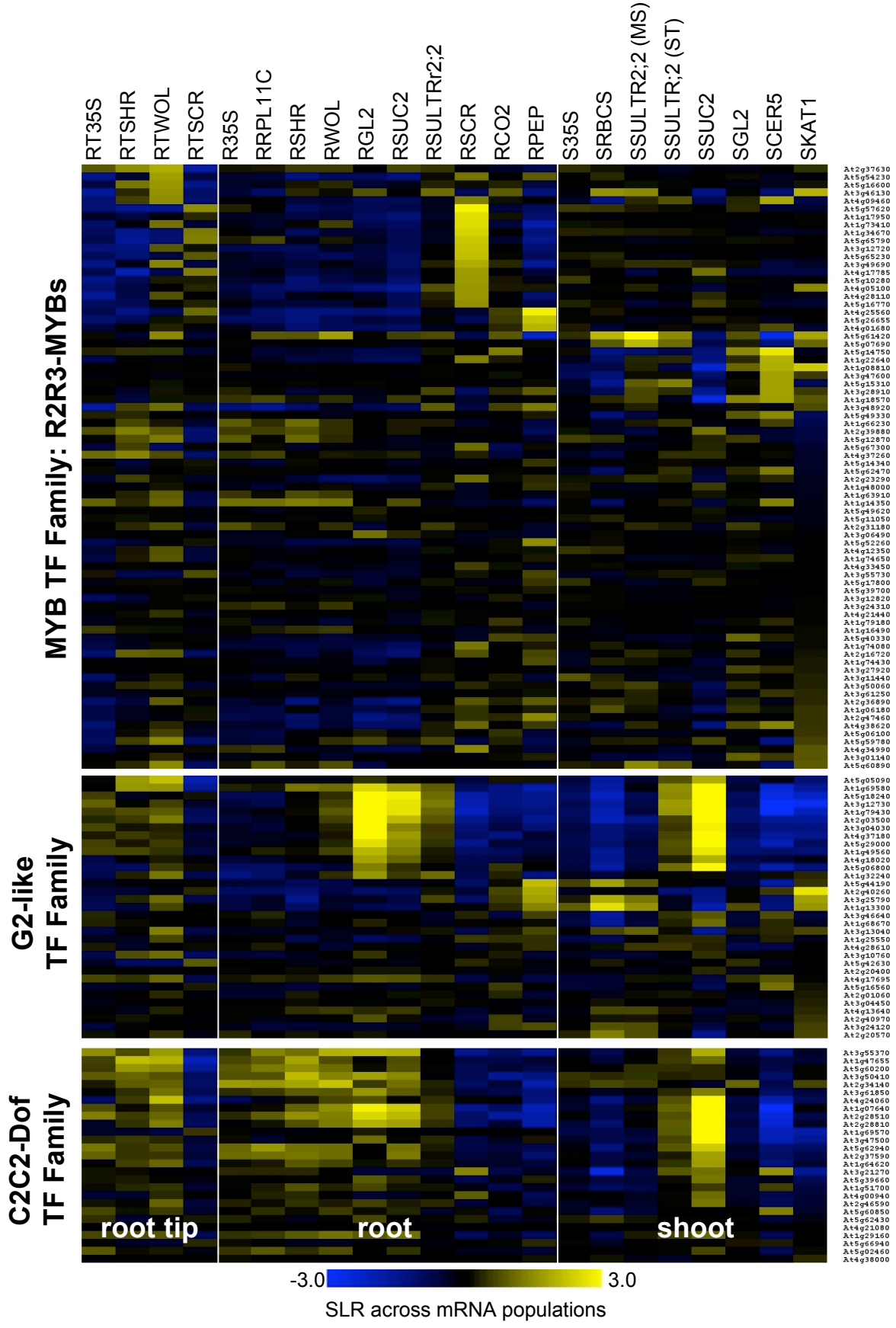
RT35S
RTSHR
RTWOL
RTSCR
R35S
RRPL11C
RSHR
RWOL
RGL2
RSUC2
RSULTRr2;2
RSCR
RCO2
RPEP
S35S
SRBCS
SSULTR2;2 (MS)
SSULTR;2 (ST)
SSUC2
SGL2
SCER5
SKAT1
MYB TF Family: R2R3-MYBs
G2-like TF Family
C2C2-Dof TF Family
root tip
root
shoot
-3.0
3.0
SLR across mRNA populations

Fig. S12C and D

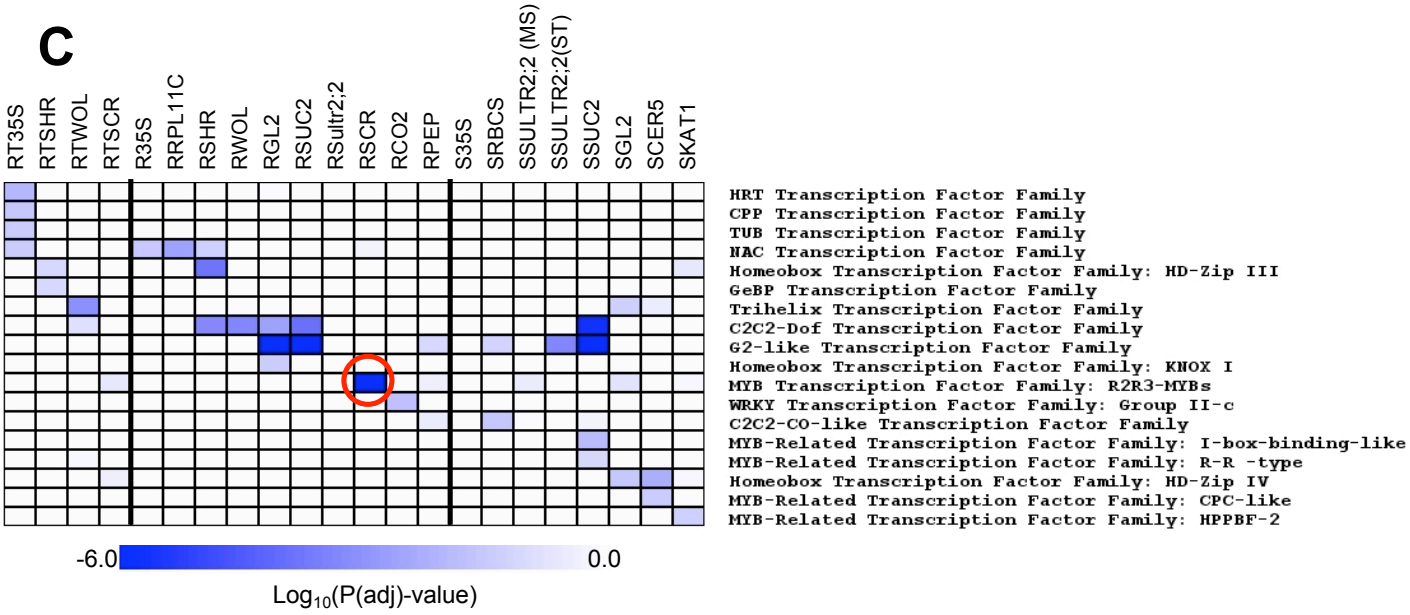

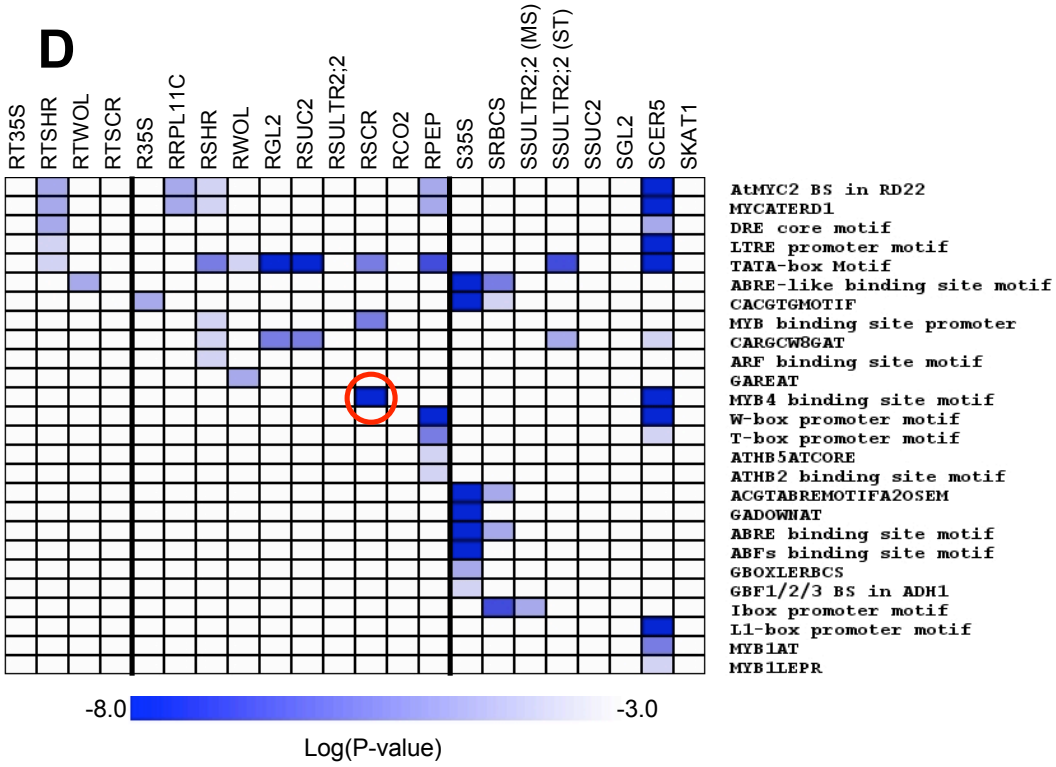

Fig. S13. Changes in expression of transcription factors during hypoxic stress. (*A*) Some transcription factor families are differentially expressed in response to hypoxia. All TF families are shown with SLRs of the comparison hypoxia versus control for all cell types and organs. Values were ordered by hierarchical clustering in MEV. Data values are from Dataset S5. (*B*) Two examples for TF families, extracted from *A*. Names of ERF TFs according to Nakano et al. (*42*). (*C* and *D*) TF family enrichment in cell type mRNA populations after hypoxic treatment. Hypoxia-induced genes in each cell type (Dataset S5) were evaluated for TF families. (*C*) TF family enrichment (TF family gene lists were obtained from TAIR and AGRIS) among the hypoxia-induced genes, analyzed for significant enrichment by the GOHyperGAll function (*27*). Data shown are log10 of adjusted P-values. (*D*) Enrichment of binding sites for transcription factors in -1000 bp promoter region of hypoxia-induced genes (analyzed by Athena). Data are log10 of adjusted P-values.

Fig. S13A

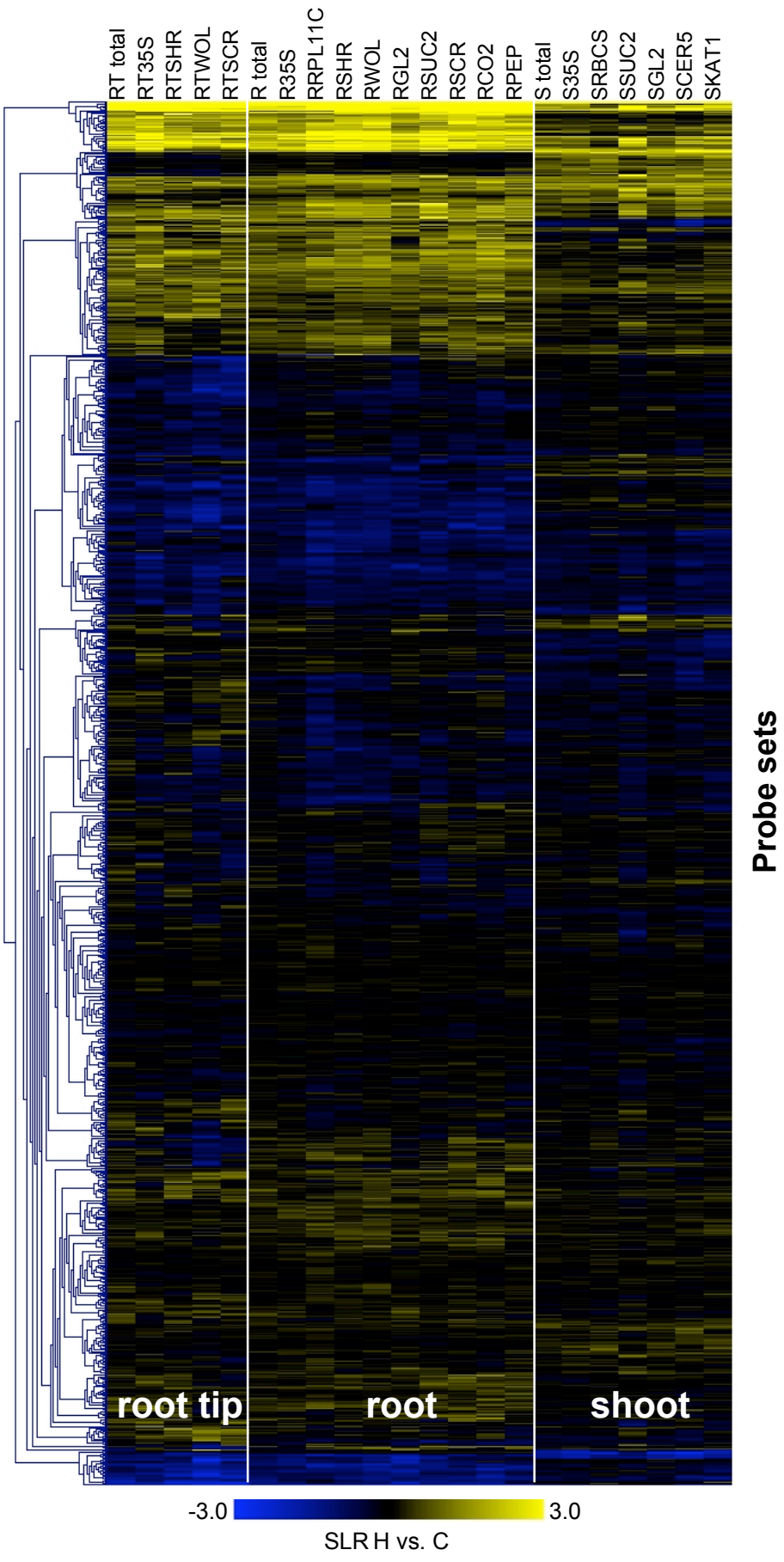
RT total
RT35S
RTSHR
RTWOL
RTSCR
R total
R35S
RRPL11C
RSHR
RWOL
RGL2
RSUC2
RSCR
RCO2
RPEP
S total
S35S
SRBCS
SSUC2
SGL2
SCER5
SKAT1
root tip
root
shoot
Probe sets
-3.0
3.0
SLR H vs. C

Fig. S13B

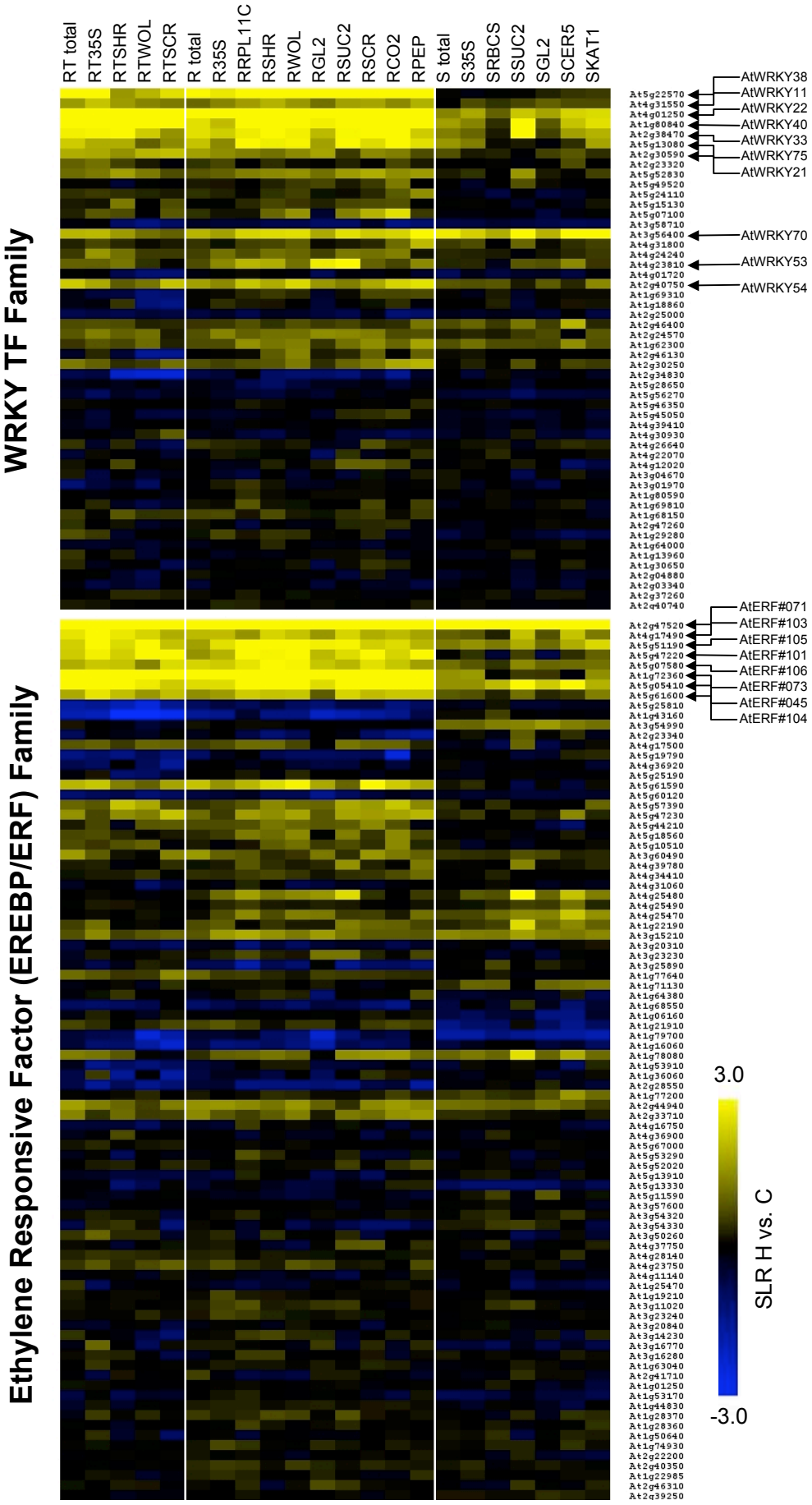
RT total
RT35S
RTSHR
RTWOL
RTSCR
R total
R35S
RRPL11C
RSHR
RWOL
RGL2
RSUC2
RSCR
RCO2
RPEP
S total
S35S
SRBCS
SSUC2
SGL2
SCER5
SKAT1
WRKY TF Family
AtWRKY38
AtWRKY11
AtWRKY22
AtWRKY40
AtWRKY33
AtWRKY75
AtWRKY21
AtWRKY70
AtWRKY53
AtWRKY54
Ethylene Responsive Factor (EREBP/ERF) Family
AtERF#071
AtERF#103
AtERF#105
AtERF#101
AtERF#106
AtERF#073
AtERF#045
AtERF#104
3.0
SLR H vs. C
-3.0

Fig. S13C, D

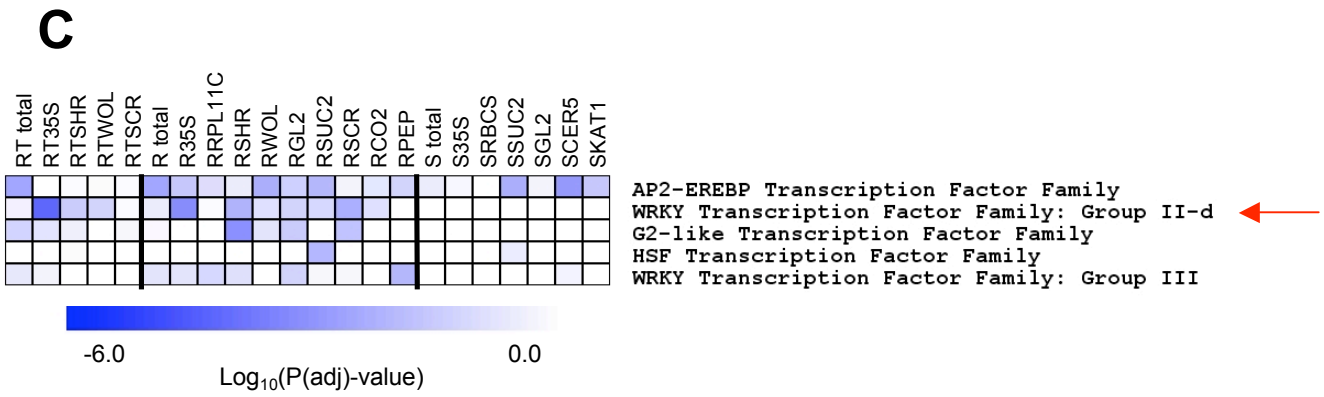
C
RT total
RT35S
RTSHR
RTWOL
RTSCR
R total
R35S
RRPL11C
RSHR
RWOL
RGL2
RSUC2
RSCR
RCO2
RPEP
S total
S35S
SRBCS
SSUC2
SGL2
SCER5
SKAT1
AP2-EREBP Transcription Factor Family
WRKY Transcription Factor Family: Group II-d
G2-like Transcription Factor Family
HSF Transcription Factor Family
WRKY Transcription Factor Family: Group III
-6.0
0.0
Log10(P(adj)-value)

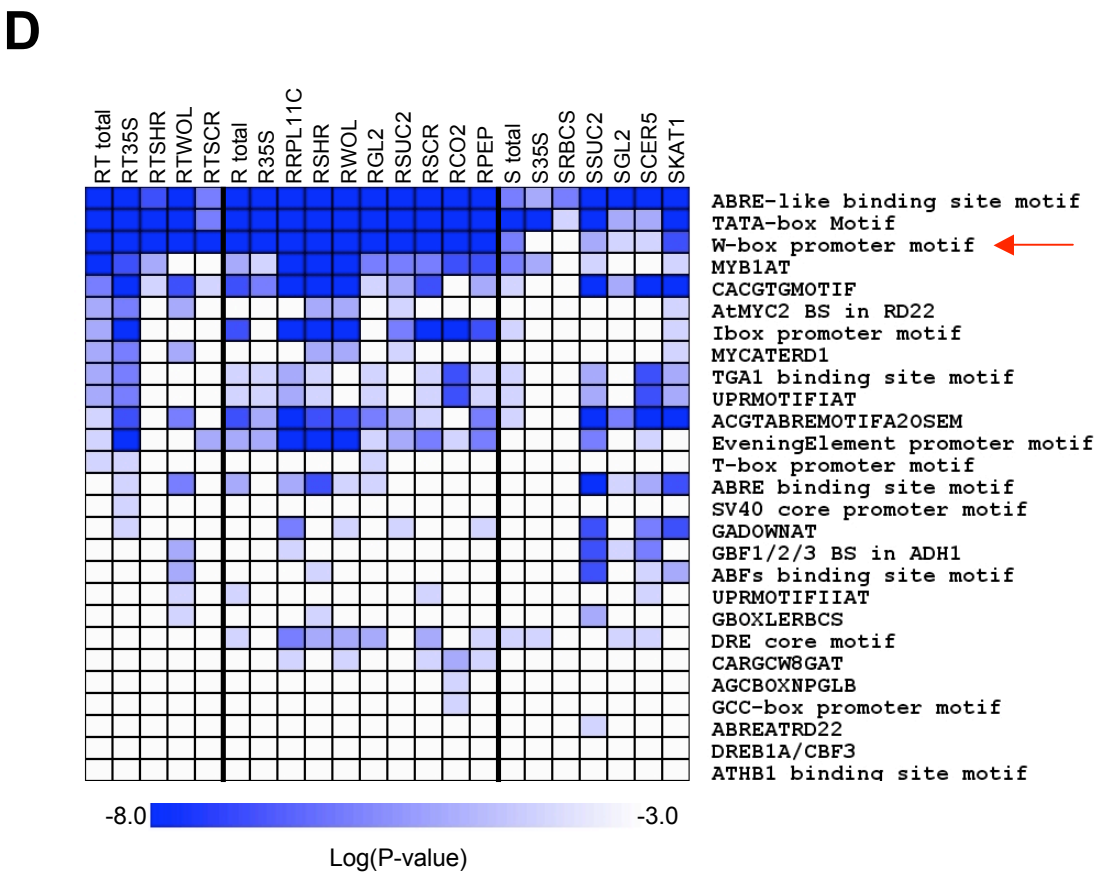
D
RT total
RT35S
RTSHR
RTWOL
RTSCR
R total
R35S
RRPL11C
RSHR
RWOL
RGL2
RSUC2
RSCR
RCO2
RPEP
S total
S35S
SRBCS
SSUC2
SGL2
SCER5
SKAT1
ABRE-like binding site motif
TATA-box Motif
W-box promoter motif
MYB1AT
CACGTGMOTIF
AtMYC2 BS in RD22
Ibox promoter motif
MYCATERD1
TGA1 binding site motif
UPRMOTIFIAT
ACGTABREMOTIFA2OSEM
EveningElement promoter motif
T-box promoter motif
ABRE binding site motif
SV40 core promoter motif
GADOWNAT
GBF1/2/3 BS in ADH1
ABFs binding site motif
UPRMOTIFIIAT
GBOXLERBCS
DRE core motif
CARGCW8GAT
AGCBOXNPGLB
GCC-box promoter motif
ABREATRD22
DREB1A/CBF3
ATHB1 binding site motif
-8.0
-3.0
Log(P-value)

Fig. S14. Plasticity in transcription factor mRNAs - ribosome association: Cell specificity and hypoxic induction. (*A*) Levels of polysomal mRNA of 1,200 expressed TFs in 7-d-old seedlings under control and hypoxia stress. TF order was organized by hierarchical clustering in MEV. Data values are scaled RMA normalized data, with control (*Left*) and hypoxia (*Right*) data shown in paired columns for each promoter used to obtain a specific mRNA population. (*B*) Level of induction of transcription factors, organized by TF families, in 7-d-old seedlings under hypoxia stress. Data values are signal-log-ratios of hypoxic versus control expression for each translatome and were organized by hierarchical clustering in MEV.

Fig. S14A

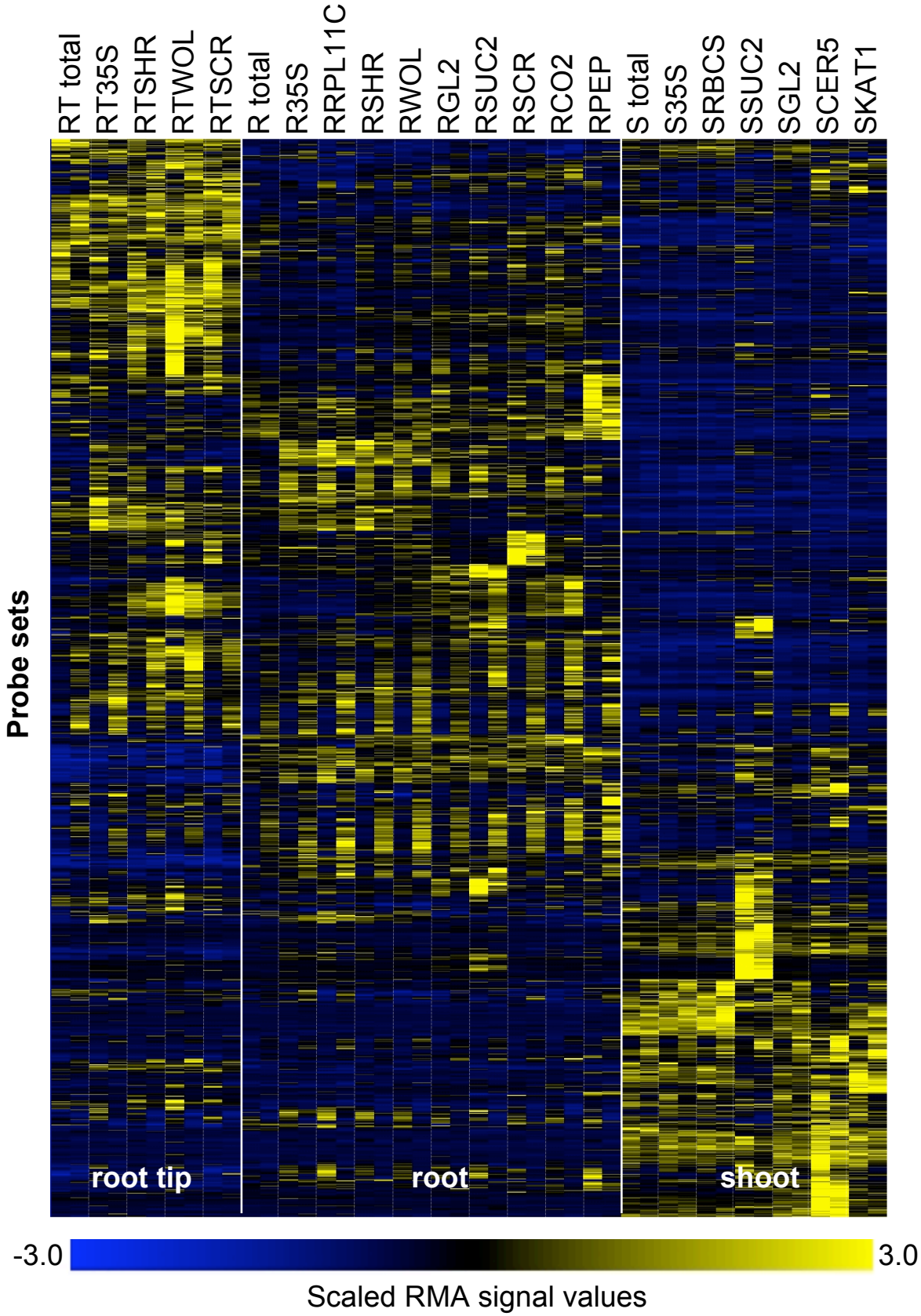
RT total
RT35S
RTSHR
RTWOL
RTSCR
R total
R35S
RRPL11C
RSHR
RWOL
RGL2
RSUC2
RSCR
RCO2
RPEP
S total
S35S
SRBCS
SSUC2
SGL2
SCER5
SKAT1
Probe sets
root tip
root
shoot
-3.0
3.0
Scaled RMA signal values

Fig. S14B

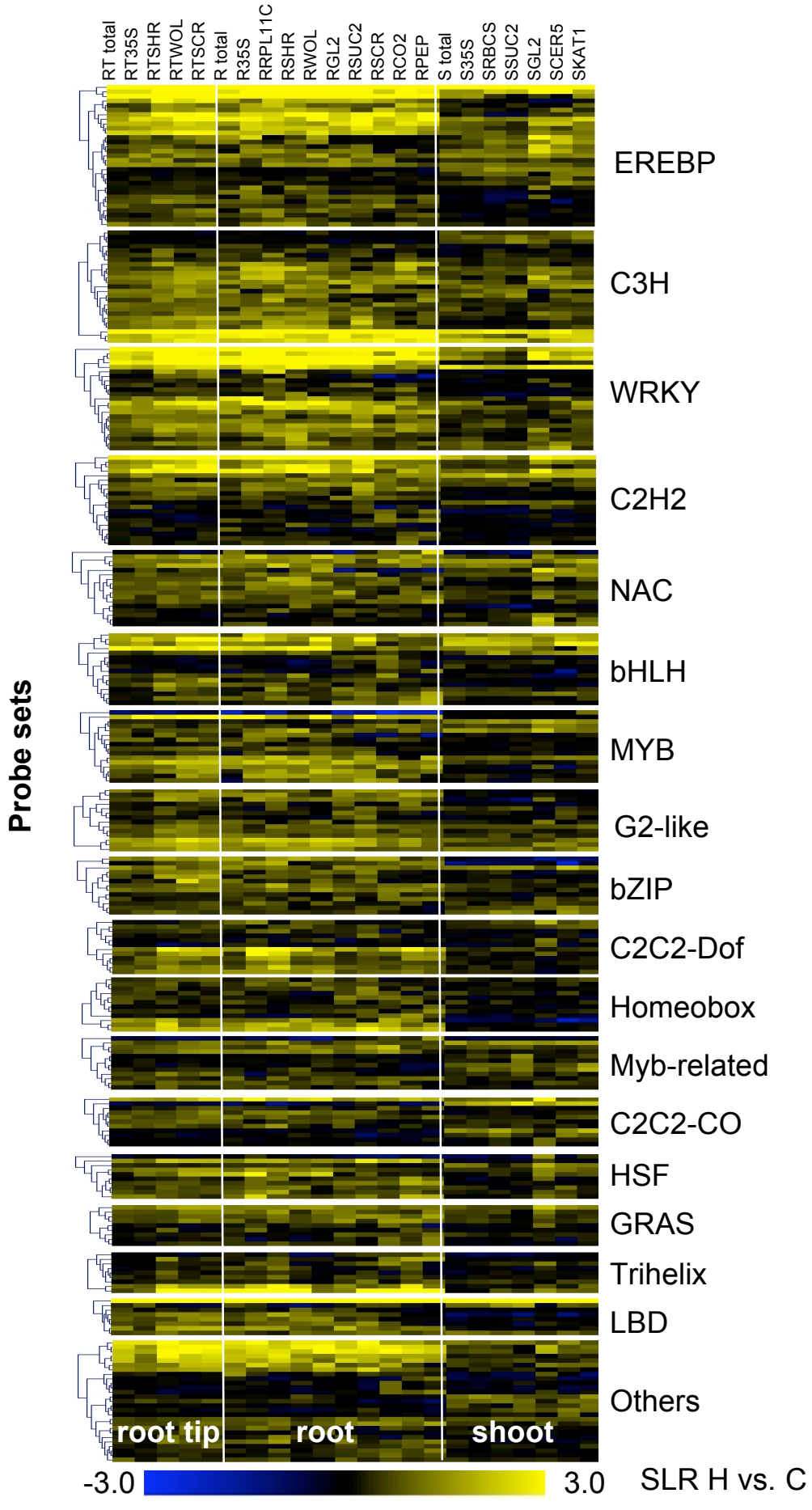
RT total
RT35S
RTSHR
RTWOL
RTSCR
R total
R35S
RRPL11C
RSHR
RWOL
RGL2
RSUC2
RSCR
RCO2
RPEP
S total
S35S
SRBCS
SSUC2
SGL2
SCER5
SKAT1
EREBP
C3H
WRKY
C2H2
NAC
bHLH
MYB
G2-like
bZIP
C2C2-Dof
Homeobox
Myb-related
C2C2-CO
HSF
GRAS
Trihelix
LBD
Others
Probe sets
root tip
root
shoot
-3.0
3.0
SLR H vs. C

Fig. S15. Immunopurified polysomal mRNA populations are distinct in organs and regions of seedlings. Robust Multi-chip Average (RMA)-normalized expression values of the 129 ATH1 GeneChips used in this study were grouped by hierarchical clustering, based on Pearson correlation distance. Individual samples clustered first by organ, then by treatment, and then by cell type, except in the shoot, where some mRNA populations (*pSUC2, pCER5, pKAT1*) clustered first by cell type, and then by treatment. All biological replicates grouped together. Sample labels are organ (R, root; RT, root tip; S, shoot; WS, whole seedling) followed by the promoter used to drive FLAG-RPL18 or Tot (total mRNA), and bioreplicate number (1-3). Whole seedling data from Branco-Price et al. (*6*) which evaluated four treatments (2hH, 2 h hypoxia; 9hH, 9 h hypoxia; R, 2hH plus 1 h reoxygenation) and two mRNA populations (T, total mRNA or 35S, immunopurified). Red arrows indicate branches that separate treatments. Promoter abbreviations correspond to names in Table 1.

Fig. S15

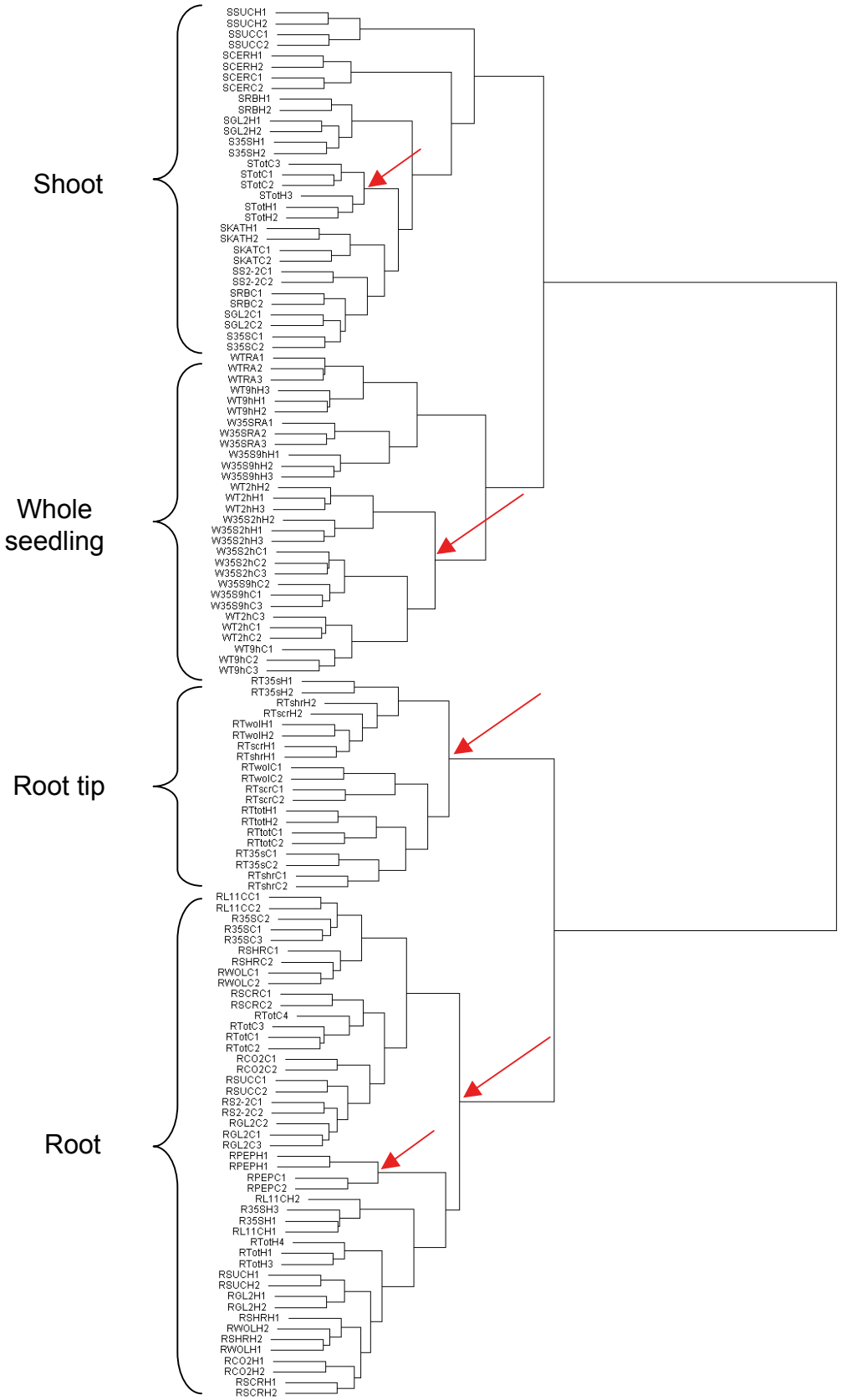
Shoot
Whole seedling
Root tip
Root
SSUCH1
SSUCH2
SSUCC1
SSUCC2
SCERH1
SCERH2
SCERC1
SCERC2
SRBH1
SRBH2
SGL2H1
SGL2H2
S35SH1
S35SH2
STotC3
STotC1
STotC2
STotH3
STotH1
STotH2
SKATH1
SKATH2
SKATC1
SKATC2
SS2-2C1
SS2-2C2
SRBC1
SRBC2
SGL2C1
SGL2C2
S35SC1
S35SC2
WTRA1
WTRA2
WTRA3
WT9hH3
WT9hH1
WT9hH2
W35SRA1
W35SRA2
W35SRA3
W35S9hH1
W35S9hH2
W35S9hH3
WT2hH2
WT2hH1
WT2hH3
W35S2hH2
W35S2hH1
W35S2hH3
W35S2hC1
W35S2hC2
W35S2hC3
W35S9hC2
W35S9hC1
W35S9hC3
WT2hC3
WT2hC1
WT2hC2
WT9hC1
WT9hC2
WT9hC3
RT35sH1
RT35sH2
RTshrH2
RTscrH2
RTwolH1
RTwolH2
RTscrH1
RTshrH1
RTwolC1
RTwolC2
RTscrC1
RTscrC2
RTtotH1
RTtotH2
RTtotC1
RTtotC2
RT35sC1
RT35sC2
RTshrC1
RTshrC2
RL11CC1
RL11CC2
R35SC2
R35SC1
R35SC3
RSHRC1
RSHRC2
RWOLC1
RWOLC2
RSCRC1
RSCRC2
RTotC4
RTotC3
RTotC1
RTotC2
RCO2C1
RCO2C2
RSUCC1
RSUCC2
RS2-2C1
RS2-2C2
RGL2C2
RGL2C1
RGL2C3
RPEPH1
RPEPH1
RPEPC1
RPEPC2
RL11CH2
R35SH3
R35SH1
RL11CH1
RTotH4
RTotH1
RTotH3
RSUCH1
RSUCH2
RGL2H1
RGL2H2
RSHRH1
RWOLH2
RSHRH2
RWOLH1
RCO2H1
RCO2H2
RSCRH1
RSCRH2

Table 1. Primers used

Primer name	Sequence (5' → 3')
Cloning	
SHR fw	CACCGGACAAAGAAGCAGAGCGTGG
SHR rev	TTAATGAATAAGAAAATGAATAGAAGAAAGGGAGACCCAC
SCR fw	CACCGGATAAGGGATAGAGGAAGAGG
SCR rev	GGAGATTGAAGGGTTGTTGGTCG
WOL fw	CACCTACTGTCTCTAAGCGCACG
WOL rev	CTGAGCTACAACAATAGAGAACAAAAGAAG
SULTR2;2 fw	CACCGACCAAAGAATCCTACGTACC
SULTR2;2 rev	GTGGGTTATTGAAGTGTGTGATAGGG
CER5 fw	CACCTTTAGTTTGCTTGAGTTCTCATGGAAG
CER5 rev	TGTTTTTGTTTGATCTTGAAAAAGATC
CO2 fw	CACCTAACTCCATTATTTACGACTGTGCCAC
CO2 rev	AAACTCTTGTTGCATTATTGTCAAATCCTT
GL2 fw	CACCGTTTCCTTCACTATACGTCTTCGTCC
GL2 rev	CTGTCCCTAGCTAGCTTCTTTGC
RBCS1A fw	CACCCCTTACGAGGAGCTTGAGCTTCAATG
RBCS1A rev	GTTCTTCTTTACTCTTTGTGTGACTGAGG
KAT1 fw	CACCTCTCATATAAATCATGCCGACATTACAC
KAT1 rev	AGAGATCGACATCTTTTTGATGATCT
PEP fw	CACCCGATGTTCACCATGCAAAAGT
PEP rev	GGTTTTGGCTAATGTGATTGTGTAGA
SUC2 fw	CACCAAGTTACTTTCTATTATTAACTGTTATAATGG
SUC2 rev	ATTTGACAAACCAAGAAAGTAAGAAAAAAAAG
sGFP fw	GACTGGATCCATGGTGAGCAAGGGCGAGGAG
sGFP rev	GTCAGGATCCCTTGTACAGCTCGTCCATGCC
Omega-KpnI fw	CGACGGTACCTATTTTTACAACAATTACCAACAAC
L18-XbaI rev	GCTCTAGATTAAACCTTGAATCCACGACTC
Tail PCR	
RB1 (step 1)	TCATGTCATAGCTGTTTCCTGTGTG
RB2 (step 2)	CTGTGTGAAATTGTTATCCGCTCAC
RB3 (step 3)	AGCCGGAAGCATAAAGTGTAAAGC
Kan1 (step 1)	CTATCAGGACATAGCGTTGGCTACC
Kan2 (step 2)	CTACCCGTGATATTGCTGAAGAGC
Kan3 (step 3)	CTTCTATCGCCTTCTTGACGAGTTC
AD1	NTCGASTWTSGWGTT
AD2	NTGCGASWGANAWGAA
AD3	WGTGNAGWANCANAGA
AD4	STTGNTASTNCTNTGC
AD5	TGWGNAGSANCASAGA
AD6	AGWGNAGWANCAWAGG
AD7	AWGCANGNCWGANATA
AD8	CGSATSTCSAANAAWAT
AD9	CGTGNAGWANCNAAG
AD10	NCTAGWASTWGSTTG
AD11	NTGGCGWSATNTSATA
AD12	NWGSTTMGAACNCGCT
AD13	SSTGGSTANATWATWCT
AD14	WCGWWGAWCANGNCGA
AD15	WGCNAGTNAGWANAAG
AD16	WGGWANCWGAWANGCA

Table 2. Characterization of T-DNA insertion sites in homozygous *p:FLAG-RPL18* lines

Transgenic Line	Target Cell Population	Promoter reference	AGI of promoter source	Length of 5' flanking region from the initiator ATG per TIGR (bp)	Line used for array studies	Chromosome of T-DNA insertion (AGI framework site)	AGI locus at or near T-DNA insertion	Orientation of transgene relative to AGI locus near insertion	Hybridizations root tip	Hybridizations root	Hybridizations shoot
p35S:FLAG-RPL18	Near constitutive (total RNA)	[*8*]		1,343	12-2-1	Chr5 (24334454)	3' of At5g60460	reverse	2xC, 2xH	4xC, 3xH	3xC, 3x
p35S:FLAG-RPL18	Near constitutive (IP'd RNA)	[*8*]		1,343	12-2-1	Chr5 (24334454)	3' of At5g60460	reverse	2xC, 2xH	3xC, 2xH	2xC, 2x
pSCR:FLAG-RPL18	Root endodermis, quiescent center	[*31*]	At3g54220	2,118	19-8-3	Chr3 (12603473)	5' flanking At3g30842	reverse	2xC, 2xH	2xC, 2xH	
pSHR:FLAG-RPL18	Root vasculature	[*32*]	At4g37650	2,505	10-1-2	Chr1 (5484948)	First intron of At1g15960	reverse	2xC, 2xH	2xC, 2xH	
pWOL:FLAG-RPL18	Root vasculature	[*33*]	At2g01830	2,085	7-1-1	Chr3 (22701280)	Within At3g61300	forward	2xC, 2xH	2xC, 2xH	
pGL2:FLAG-RPL18	Root atrichoblast epidermis, shoot trichomes[1]	[*1,2*]	At1g79840	2,059	38-4	Chr3 (18988245)	3' of At3g51090	forward		2xC, 2xH	2xC, 2x
pGL2:FLAG-RPL18[2]	Root atrichoblast epidermis, shoot trichomes[1]	[*1,2*]	At1g79840	2,059	16-4	Chr4 (7992964)	5' flanking At4g13770	forward		1xC[2]	
pCO2:FLAG-RPL18	Root cortex meristematic zone	[*34*]	At1g62500	586	1-7	ND					
pPEP:FLAG-RPL18	Root cortex elongation and maturation zone	[*35*]	At1g09750	1,667	5-11	Chr4 (10801442)	5' flanking At4g19925	reverse		2xC, 2xH	2xC, 2x
pRPL11C:FLAG-RPL18	Root proliferating cells	[*36*]	At4g18730	1,000	10-1-2	Chr5 (24334451)	3' of At5g60460	reverse		2xC, 2xH	
pSUC2:FLAG-RPL18	Root and shoot phloem companion cells	[*37*]	At1g22710	2,097	16-8	ND[3]				2xC, 2xH	
pSULTR2;2:FLAG-RPL18	Root phloem companion cells, shoot bundle sheath	[*3*]	At1g77990	1,962	1-3-9	Chr3 (10009685)	5' flanking At3g27140	reverse		2xC	
pCER5:FLAG-RPL18	Cotyledon and leaf epidermis	[*38*]	At1g51500	2,614	25-2	Chr1 (19224463); Chr1 (6771552)	3' of At1g51805; 5' flanking At1g19560	reverse; reverse			2xC, 2x
pKAT1:FLAG-RPL18	Cotyledon and leaf guard cells	[*39*]	At5g46240	3,410	23-4	ND					2xC, 2x
pRBCS:FLAG-RPL18	Shoot photosynthetic	[*40*]	At1g67090	1,976	9-11	Chr3 (<519301)	5' of At3g02500	forward			

p35S: *Cauliflower mosaic virus 35S*; *pRPL11C*, *RIBOSOMAL PROTEIN L11C; pSCR, SCARECROW; pWOL, WOODENLEG; pSUC2, SUCROSE TRANSPORTER 2; pSULTR2;2, SULPHATE TRANSPORTER 2*; *pGL2, GLABRA*2; *pCO2,* Cortex specific transcript; *pPEP*, plastid endopeptidase; *pRBCS1A, RIBULOSE BISPHOSPHATE CARBOXYLASE SMALL CHAIN 1A*; *pCER5, ABC TRANSPORTER ABCG SUBFAMILY 12*; *pKAT1, POTASSIUM CHANNEL IN ARABIDOPSIS THALIANA 1*. C, control treatment; H, 2 h hypoxia stress treatment; ND, insertion was not successfully determined by TAIL-PCR or inverse PCR. [1]*pGL2* was expressed in the targeted cell population as well as in the phloem companion cells. [2]Hybridization with RNA from a second independent transgenic line with the insertion site of T-DNA in a different genomic location. [3]Insertion was defined as two side-by-side insertions of the T-DNA but Tail-PCR inside genomic region was not possible.

Supplemental Datasets

Dataset S1 (XLS): Normalized Microarray Data. Sheet *a*, Present calls. PMA values, obtained by use of the MAS5 algorithm in R, were transformed into numerical values as follows: 0=A=absent; 1=M=marginal; 2=P=present. The mean of the PMA value was calculated for the biological replicates for each probe pair set. The maximum number across all samples (root, shoot, root tip, C and H, all cell types) was recorded and shows if a gene was present in at least one sample set. For all subsequent analyses and tables we excluded the 219 organelle-encoded genes and the 5,123 genes that did not have at least one P (=maxP<2) across all sample sets. Sheet *b*, List of 6657 genes with a present call in all samples. Sheet *c*, GO term enrichment of genes from sheet *b*. Sheet *d*, The mean of RMA normalized expression values was calculated for the replicates. Sheet *e*, The mean of RMA normalized expression values, unlogged. Sheet *f*, Correlation coefficients (R^2 values) from comparison of RMA normalized signal values from individual hybridizations. Values highlighted in yellow compare biological replicate samples.

Dataset S2 (XLS): Differential Gene Expression Analysis of mRNA Populations from Different Cell Types. Sheets *a*--*e*, The goal of the comparison was to identify genes transcripts that are enriched in specific mRNA populations as compared to other populations isolated from the same organ or region. RMA raw data were used to perform comparisons between cell types by use of LIMMA (R). Within one organ, non-overlapping cell types were compared (see sheet *b* "queries" for the specific comparisons). Comparisons were done only for the control (C) data, and separately for hypoxia data. For some cell types (vasculature in roots, epidermis and vasculature in shoots), two different stringencies were applied (sheet *e*, "additional queries"). Selection criteria for significantly enriched gene transcripts for each pairwise comparison: >2-fold change; FDR <0.01. The number of significantly enriched genes found in each pairwise comparison is given in sheet *d*. The overlap of the pairwise

comparisons was recorded. Individual columns in sheet *a* indicate the genes that were significantly higher or lower in the mRNA population sampled with a specific *p:FLAG-RPL18* construct. Additionally, the mean of the SLRs and the mean of the FDRs of all utilized comparisons were calculated. Sheet *c* contains numbers of enriched or depleted genes for each cell type and comparison variant, and additional comparisons to literature cell-type data (*21*--*25*). Sheets *f*--*k*, GO and TF family enrichment analysis of enriched gene lists for different cell types. GO term enrichment was calculated with the GOHyperGAll function (*27*). First, all GOs that were significantly enriched in a gene list (Padj<0.05) were recorded. Second, the overlapping GO categories were reduced to remove nested GO terms with the Simplify variant of the GOHyperGAll function. TF enrichment was calculated accordingly, after obtaining TF family gene lists from TAIR and AGRIS (*30*). Clusters with fewer than 10 genes were not evaluated for GO enrichment. Sheet *k*, log-transformed adjusted P-values of GO term enrichment that were used to make Fig. 2*B* and Fig. S6.

Dataset S3 (XLS): Analysis to Identify Genes That Are Enriched in Multiple Cell Types (Sampled mRNA Populations). Fuzzy k-means clustering was done with the mean of replicates of RMA normalized values, after filtering out low-varying genes, by use of the FANNY function with the following settings: membership exponent = 1.1, cluster number = 60, cluster collapsing with HC = 0.05, membership coefficients cut off (probability to belong to a cluster) = 0.4. Clustering was done for control (C) data, and separately for hypoxia (H) data. For control samples, 17,468 genes were used for filtering, 11,273 genes were used for clustering, 257 genes did not belong to any cluster, and 362 genes belong to two clusters. Scaled values of RMA normalized data are added for easier visualization of cluster patterns, as well as median expression values of each cluster are presented in sheet *b*. Data were used to prepare Fig. 2. Sheets *c* and *d*, GO and TF family enrichment analysis of fuzzy clusters. GO term enrichment was calculated with the GOHyperGAll function (*27*). First, all GOs that

were significantly enriched in a gene list (Padj<0.05) were recorded. Second, the overlapping GO categories were reduced to remove nested GO terms with the Simplify variant of the GOHyperGAll function. TF enrichment was calculated accordingly, after obtaining TF family gene lists from TAIR and AGRIS (30). Clusters with fewer than 10 genes were not evaluated for GO enrichment.

Dataset S4 (XLS): Comparison of Significantly Enriched mRNAs in mRNA Populations Determined by Others, and This Study. Gene lists from the present study are from Dataset S2, and are labeled with (A). Literature gene lists are from the following sources, and labeled with (B): root cell types (*25*); shoot epidermis (*21*); guard cells (*22*); trichomes (*23*); shoot vasculature (*24*). For all experiments, published .CEL files were used for a new RMA analysis to compare cell type samples to references samples (or to non-overlapping root cell types for ref. *25* according to the queries defined in sheet c) by LIMMA, regardless of different treatments, by use of the selection criteria >2-fold change; FDR <0.01. For each of the gene lists, GO enrichment was analyzed by the function GOHyperGALL (*27*). The overlap between enriched GO lists for each comparison was determined and recorded in this file. Sheets *a*--*c*: root cell types; sheets *d*--*e*: shoot cell types.

Dataset S5 (XLS): Differential Expression Analysis of the Hypoxic Response. RMA raw data were used to do comparisons between H and C by use of LIMMA (R). Sheet *a* and *b*, For each cell type, a comparison of hypoxia versus control was performed, and the SLR and FDR were calculated. Genes that were significantly changed due to hypoxic stress were selected with the criteria: >2-fold change; FDR <0.01. The "Core" response (ubiquitous hypoxia-response) genes were defined as genes that were significantly induced or reduced in all cell types of an organ. Sheet *a* shows number of hypoxia induced or reduced genes for each cell type. Sheets *c*--*f*, GO and TF family enrichment analysis of the hypoxic response. GO term

enrichment was calculated with the GOHyperGAll function (*27*). First, all GOs that were significantly enriched in a gene list (Padj<0.05) were recorded. Second, the overlapping GO categories were reduced to remove nested GO terms with the Simplify variant of the GOHyperGAll function. Enriched GO terms of hypoxia induced genes that occur in multiple cell types are marked with blue. TF enrichment was calculated accordingly, after obtaining TF family gene lists from TAIR and AGRIS (*30*). Clusters with fewer than 5 genes were not evaluated for GO enrichment. Sheet *g*, log-transformed adjusted P-values for GO term enrichment that were used to make Fig. S9. Sheets *h*--*l*, "reduced genes": selection of genes that show cell specificity under control conditions (see Dataset S2 for details) AND are significantly reduced under H in that cell type. Sheets *m*--*o*, "hypoxic genes": selection of genes that show cell specificity under control conditions (see Dataset S2 for details) AND are hypoxia-induced in total RNA in the same organ.

Dataset S6 (XLS): Analysis to Identify Genes that are Differentially Changed During Hypoxia Between Cell Types (Sampled mRNA Populations). Sheets *a* and *b*, Fuzzy k-means clustering was done with the mean of replicates of RMA normalized values, by use of the FANNY function with the following settings: membership exponent = 1.1, cluster number = 100, cluster collapsing with HC = 0.05, membership coefficients cut off (probability to belong to a cluster) = 0.4. For clustering, only genes were selected that showed significant up- or down-regulation due to hypoxia in any cell type or organ (see Dataset S5 for details). 6,461 genes were used for clustering, 255 genes did not belong to any cluster, and 174 genes belong to two clusters. Scaled values of RMA normalized data are added for easier visualization of cluster patterns, as well as median expression values of each cluster are presented in sheet *b*. Data were used to prepare Fig. 3. Sheets *c* and *d*, For each cluster from fuzzy-k-mean clustering, GO term enrichment was analyzed with the GOHyperGAll function (*27*). First, all GOs that were significantly enriched in a gene list (Padj<0.05) were recorded. Second, the

overlapping GO categories were reduced to remove nested GO terms with the Simplify variant of the GOHyperGAll function. TF enrichment was calculated accordingly, after obtaining TF family gene lists from TAIR and AGRIS (*30*). Clusters with fewer than 10 genes were not evaluated for GO enrichment.

Dataset S7 (XLS): Differential Gene Expression Analysis of SLR H vs. C Between Cell Types. Sheets *a--d*, The goal of the comparison was to identify genes transcripts that are differentially changed due to hypoxia in specific mRNA populations as compared to other populations isolated from the same organ or region. RMA raw data were used to do comparisons between cell types AND stresses by use of LIMMA (R) and the following formula: (CT(hypoxia)-CT(control))-(ref(hypoxia)-ref(control)), while "ref" means all non-overlapping cell types (comparisons see sheet *b* "queries"). Selection criteria for significantly enriched gene transcripts for each pairwise comparison: >2-fold change; FDR <0.01. The number of significantly enriched genes for each cell type is given in sheet *c*. The overlap of all gene lists was recorded. Individual columns in sheet *a* indicate the genes that were significantly higher or lower induced during hypoxia in the mRNA population sampled with a specific *p:FLAG-RPL18* construct. Additionally, the mean of the SLRs and the mean of the FDRs of all utilized comparisons were calculated. Sheet *d* contains numbers of enriched or depleted genes for pairwise comparison. Sheets *e--h*, GO and TF family enrichment analysis of the cell-type specific hypoxic response. GO term enrichment was calculated with the GOHyperGAll function (*27*). First, all GOs that were significantly enriched in a gene list (Padj<0.05) were recorded. Second, the overlapping GO categories were reduced to remove nested GO terms with the Simplify variant of the GOHyperGAll function. TF enrichment was calculated accordingly, after obtaining TF family gene lists from TAIR and AGRIS (*30*). Clusters with fewer than 10 genes were not evaluated for GO enrichment.